Article

Cell Reports

Prdm12 Directs Nociceptive Sensory Neuron Development by Regulating the Expression of the NGF Receptor TrkA

Graphical Abstract

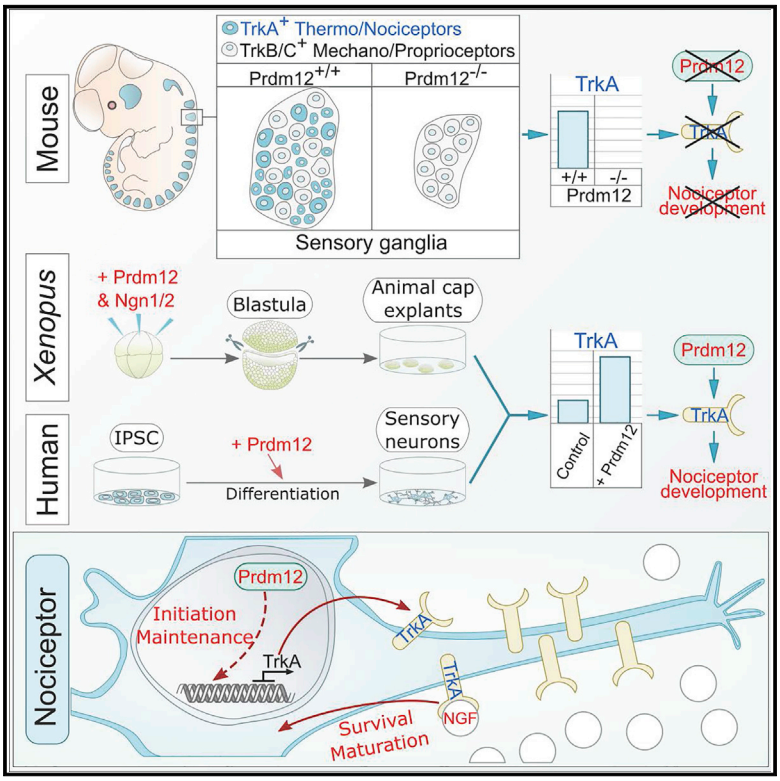

Highlights

- In somatosensory ganglia, Prdm12 is specific to the nociceptive lineage
- Prdm12 is necessary for the survival of developing nociceptors
- Prdm12 initiates and maintains the expression of TrkA in developing nociceptors
- Prdm12 acts in conjunction with bHLH proteins Ngn1/2 to promote a nociceptor fate

Authors

Simon Desiderio, Simon Vermeiren, Claude Van Campenhout, ..., Vanja Nagy, Catherine Verfaillie, Eric J. Bellefroid

Correspondence

ebellefr@ulb.ac.be

In Brief

Desiderio et al. report that, in developing somatosensory neurons, *Prdm12* is restricted to the nociceptors and that these are selectively eliminated from *Prdm12* mutant mice. In *Xenopus* and human iPSCs, they show that Prdm12, in conjunction with bHLH proneural proteins, promotes the expression of the neurotrophin receptor TrkA.

Desiderio et al., 2019, Cell Reports *26*, 3522–3536
March 26, 2019
https://doi.org/10.1016/j.celrep.2019.02.097

CellPress

OPEN ACCESS
CellPress

Cell Reports
Article

Prdm12 Directs Nociceptive Sensory Neuron Development by Regulating the Expression of the NGF Receptor TrkA

Simon Desiderio,[1,9] Simon Vermeiren,[1,9] Claude Van Campenhout,[1] Sadia Kricha,[1] Elisa Malki,[1,2] Sven Richts,[4] Emily V. Fletcher,[3] Thomas Vanwelden,[2] Bela Z. Schmidt,[2] Kristine A. Henningfeld,[4] Tomas Pieler,[4] C. Geoffrey Woods,[3,5] Vanja Nagy,[6,7,8,10] Catherine Verfaillie,[2,10] and Eric J. Bellefroid[1,10,11,*]

[1]ULB Neuroscience Institute (UNI), Université Libre de Bruxelles (ULB), 6041 Gosselies, Belgium
[2]KU Leuven, Interdepartmental Stem Cell Institute, Department of Development and Regeneration, Stem Cell Biology and Embryology, 3000 Leuven, Belgium
[3]Cambridge Institute for Medical Research, University of Cambridge, CB2 0QQ Cambridge, UK
[4]Institute of Developmental Biochemistry, Center for Nanoscale Microscopy and Molecular Physiology of the Brain (CNMPB), University of Goettingen, 37077 Goettingen, Germany
[5]Department of Medical Genetics, University of Cambridge, CB2 0XY Cambridge, UK
[6]Institute of Molecular Biotechnology of the Austrian Academy of Sciences (IMBA), Vienna Biocenter (VBC), 1030 Vienna, Austria
[7]Ludwig Boltzmann Institute for Rare and Undiagnosed Diseases, 1090 Vienna, Austria
[8]CeMM Research Center for Molecular Medicine of the Austrian Academy of Sciences, 1030 Vienna, Austria
[9]These authors contributed equally
[10]Senior author
[11]Lead Contact
*Correspondence: ebellefr@ulb.ac.be
https://doi.org/10.1016/j.celrep.2019.02.097

SUMMARY

In humans, many cases of congenital insensitivity to pain (CIP) are caused by mutations of components of the NGF/TrkA signaling pathway, which is required for survival and specification of nociceptors and plays a major role in pain processing. Mutations in *PRDM12* have been identified in CIP patients that indicate a putative role for this transcriptional regulator in pain sensing. Here, we show that Prdm12 expression is restricted to developing and adult nociceptors and that its genetic ablation compromises their viability and maturation. Mechanistically, we find that Prdm12 is required for the initiation and maintenance of the expression of TrkA by acting as a modulator of Neurogenin1/2 transcription factor activity, in frogs, mice, and humans. Altogether, our results identify Prdm12 as an evolutionarily conserved key regulator of nociceptor specification and as an actionable target for new pain therapeutics.

INTRODUCTION

Understanding the molecular mechanisms of cell fate specification in the neuronal lineage is a major challenge in developmental neurobiology. Among the types of neurons of the nervous system, somatosensory neurons are of particular importance, because they continuously relay information about our body's external and internal environment.

Somatosensory information from the face and the body is transmitted through specialized sensory neurons whose cell bodies are located in the trigeminal ganglia (TGs) and dorsal root ganglia (DRGs), respectively. These neurons are classified into several major types, based on different perceptual modalities. These include proprioceptors sensing body position, mechanoreceptors mediating touch, and nociceptors involved in pain, itch, and temperature perception (Basbaum et al., 2009). Each of these major functional classes is subdivided into subtypes exhibiting distinct physiological, morphological, and molecular properties (Lallemend and Ernfors, 2012; Usoskin et al., 2015).

The three major classes of DRG and TG neurons can be molecularly discriminated by their differential expression of neurotrophic receptors: tyrosine receptor kinase A (TrkA, encoded by *Ntrk1*), which responds to nerve growth factor (NGF) and is restricted to nociceptors; TrkB (encoded by *Ntrk2*), which is activated by brain-derived neurotrophic factor (BDNF) and neurotrophin 4/5 (NT4/5); and TrkC (encoded by *Ntrk3*), which activated by NT3 and expressed in mechanoreceptors and/or proprioceptors (Lallemend and Ernfors, 2012). Trk receptors and their cognate neurotrophins function to support survival, sensory subtype specification, axonal outgrowth, modality-specific target innervation, and phenotypic maturation (Harrington and Ginty, 2013).

During development, DRG neurons are generated from multipotent neural crest (NC) cells, whereas TG neurons have a dual origin from both NC and placodes (Barlow, 2002; Lallemend and Ernfors, 2012). In mice, the major classes of sensory neurons are added to the DRGs during two successive overlapping waves of neurogenesis, controlled by the activity of the proneural factors Neurogenin2 (Ngn2) and Neurogenin1 (Ngn1) that

direct NC cells to the sensory lineage (Lallemend and Ernfors, 2012; Ma et al., 1999). Between embryonic day (E) 9.5 and E11.5, the first Ngn2-mediated wave generates large myelinated Ret$^+$, Ret$^+$/TrkB$^+$, TrkB$^+$, and TrkB$^+$/TrkC$^+$ mechanoreceptors and TrkC$^+$ proprioceptors, as well as a subset of slightly myelinated small TrkA$^+$ nociceptors (eTrkA) (Bachy et al., 2011). The second Ngn1-dependent wave that occurs between E10.5 and E13.5 predominately produces unmyelinated small TrkA$^+$ nociceptive neurons (Lallemend and Ernfors, 2012). Through the postnatal period, sensory neurons of the second wave segregate into two main subpopulations: TrkA$^+$ peptidergic nociceptors that remain dependent on NGF/TrkA signaling for their full phenotypic maturation and Ret$^+$ non-peptidergic nociceptors that stop responding to NGF and become dependent on glial cell-derived neurotrophic factor (GDNF) (Denk et al., 2017; Lallemend and Ernfors, 2012; Luo et al., 2007; Marmigère and Ernfors, 2007). Among the intrinsic determinants of the sensory lineage required for sublineage specification are the Runx transcription factors. While Runx3 is involved in the differentiation of proprioceptive sensory neurons, Runx1 plays an important role in the diversification of the Ngn1-dependent TrkA embryonic lineage and is considered a master regulator of the non-peptidergic neurons (Lallemend and Ernfors, 2012; Qi et al., 2017).

In humans, many cases of congenital insensitivity to pain (CIP) are caused by mutations in *NGF* or *NTRK1*, leading to massive apoptosis of nociceptors and highlighting the importance of the NGF signaling pathway in nociceptor development and survival (Denk et al., 2017; Nahorski et al., 2015). However, despite this importance, little is known about the molecular mechanisms controlling the expression of *NGF* and its receptor. Understanding the molecular mechanisms controlling *Ntrk1* induction and maintenance in developing sensory neurons is therefore an important step in unravelling the process of nociceptive neuron specification (Lallemend and Ernfors, 2012).

PRDM12 belongs to the *PRDM* (PRDI-BF1 and RIZ homology domain-containing gene) family of genes encoding epigenetic regulators. Members of this family are important regulators of cell proliferation and differentiation in development and diseases (Fog et al., 2012; Hohenauer and Moore, 2012; Mzoughi et al., 2016). *PRDM12* is a recently discovered evolutionarily conserved member of this family. It is expressed in sensory neurons and has been found mutated in CIP patients (Chen et al., 2015; Nagy et al., 2015). However, whether PRDM12 plays an important role in nociceptors biology and, thereby in pain perception, remains unknown. Here, we show that *Prdm12* is selectively expressed in developing and mature nociceptors and establishes a genetic relationship between its expression and the survival of developing nociceptors. Mechanistically, we demonstrate that Prdm12 is required for nociceptors, mainly through its role in the initiation and maintenance of the expression of the NGF receptor TrkA. Prdm12 modulates Ngn1- and Ngn2-inducing activity, promoting their ability to induce TrkA receptor expression at the expense of the other Trk receptors in both frogs and humans. Altogether, these results establish *Prdm12* as an evolutionarily conserved master regulator of nociceptor development, acting during their specification and differentiation, through its ability to modulate the NGF signaling pathway.

RESULTS

Prdm12 Is Expressed in Somatosensory Neural Precursors and Marks Differentiating TrkA$^+$ Nociceptors

To assess the role of *Prdm12* in sensory neuron differentiation, we first examined *Prdm12* expression in the developing mouse embryo by *in situ* hybridization. In accordance with previous studies (Chen et al., 2015; Kinameri et al., 2008), *Prdm12* was detected in DRGs and cranial ganglia during embryogenesis (from E9.5) and in adult mice. In embryonic and adult DRGs, *Prdm12* expression appeared in a salt-and-pepper pattern (Figures S1A–S1D), suggesting it is restricted to a specific subtype of sensory neurons.

To identify the cell types expressing Prdm12 in the developing sensory neurons, we performed double immunostainings on head and trunk sensory ganglia at different embryonic stages. In DRGs, we first examined Prdm12 expression in relation to the NC transcription factor Pax3, the pan-sensory neuron transcription factor Islet1, and the glial transcription factor Sox10. At E11, we observed that *Prdm12* is co-expressed with Pax3 in some NC-derived progenitors, mainly found in the dorsal part of the DRGs (Figure 1A). We found Prdm12$^+$ cells co-expressing Islet1 from E9.5, and the incidence of Prdm12$^+$/Islet1$^+$ cells strongly increased from E12.5 onward (Figures 1B–1F). In contrast, we did not detect co-expression with Sox10, which is restricted to glial cells at E14.5 (Figure 1G). In the head of E9.5–E13.5 embryos, Prdm12 was also expressed in neurons of specific cranial ganglia: TGs, vestibulo-acoustic ganglia (VAGs), and superior-jugular ganglia (SJGs) (Figures S1E and S1F). No expression was detected in epibranchial ganglia (geniculate, petrosal, and nodose). In TGs, Prdm12 was co-expressed with Islet1, with the incidence of double-positive cells increasing from E9.5 to E13.5 (Figures S1G–S1I). These results indicate that Prdm12 is expressed from the somatosensory neural precursor stage during the development of a subpopulation of sensory neurons.

To determine which neuronal subtypes express *Prdm12*, we next examined in developing DRGs and TGs how it segregates with the expression of TrkA, labeling cells devoted to become nociceptors, and TrkB and TrkC, marking cells directed to the mechanoreceptive-proprioceptive fate (Lallemend and Ernfors, 2012). While virtually all TrkA$^+$ neurons co-expressed Prdm12 in E12.5 and E14.5 DRGs, TrkB$^+$ and TrkC$^+$ cells did not co-express Prdm12 (Figures 1H–1M). In TGs and SJGs, selective co-expression of Prdm12 and TrkA staining was also evident (Figures S1J–S1M). In embryonic DRGs, we also examined the relation of Prdm12 to Runx3, which controls the development of TrkC$^+$ proprioceptive neurons (Lallemend and Ernfors, 2012). Whereas a few Prdm12$^+$/Runx3$^+$ cells were present at E12.5, none were detected at E14.5 (Figures 1N and 1O). We further assessed the co-expression of Prdm12 with TrkA at E18.5 and compared it with the nociceptor-specific voltage-gated sodium channel Nav1.8 (Usoskin et al., 2015) and Runx1, which marks most TrkA$^+$ cells at E14.5 and whose expression becomes restricted during later embryonic and

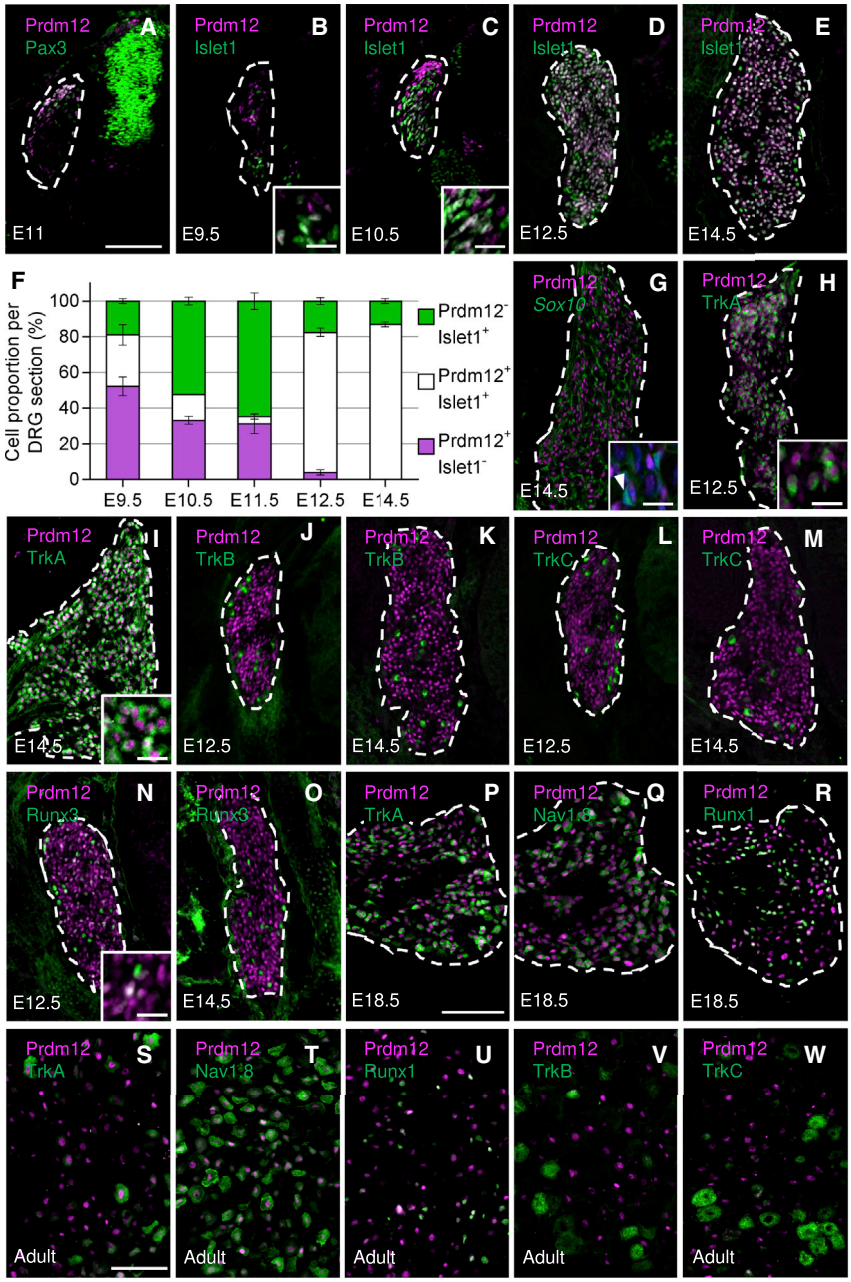

Figure 1. Prdm12 Expression in Dorsal Root Ganglia

(A–W) Transverse DRG sections of embryonic or adult mice as indicated, double immunostained with Prdm12 (purple) and the indicated markers (green).

(A) Immunostainings of Prdm12 and the neural crest transcription factor Pax3 at E11.

(B–F) Immunostainings of Prdm12 and the pan-neuronal transcription factor Islet1 at E9.5 (B), E10.5 (C), E12.5 (D), or E14.5 (E). The proportion of Prdm12+, Islet1+, or Prdm12+/Islet1+ cells detected at the different analyzed stages is shown in (F) (mean ± SD; n = 2 [E10.5], 3 [E9.5, E12.5, and E14.5], or 5 [E11.5]) embryos.

(G) Immunostaining of Prdm12 and a Sox10 reporter construct enabling the vizualisation of Sox10$^+$ satellite cells at E14.5. The inset shows a higher magnification view of an area with DAPI counterstaining (blue), and the arrowhead points to a putative Sox10$^+$ satellite cell surrounding a Prdm12$^+$ cell.

(H, I, P, and S) Immunostainings of Prdm12 with the neurotrophic receptor TrkA at E12.5 (H), E14.5 (I), E18.5 (P), or in adult DRG (S).

(J, K, and V) Immunostainings of Prdm12 with the neurotrophic receptor TrkB at E12.5 (J), E14.5 (K), or in adult DRG (V).

(L, M, and W) Immunostainings of Prdm12 with the neurotrophic receptor TrkC at E12.5 (L), E14.5 (M), or in adult DRG (W).

(N–O) Immunostainings of Prdm12 with the transcription factor Runx3 at E12.5 (N) or E14.5 (O).

(Q–T) Immunostainings of Prdm12 with the nociceptor specific ion channel Nav1.8 at E18.5 (Q) or in adult DRG (T).

(R–U) Immunostainings of Prdm12 with the transcription factor Runx1 at E18.5 (R) or in adult DRG (U).

In (B), (C), (H), (I), and (N), the insets are higher magnification views of a selected area demonstrating the extensive overlap of the Prdm12 staining with the second marker. DRGs are delineated with dashed lines. Scale bars in main pictures, 100 μm; scale bars in magnified pictures, 25 μm.

See also Figure S1.

postnatal stages to the non-peptidergic subset of nociceptors (Lallemend and Ernfors, 2012). At this stage, 86.2% ± 13.7% (mean ± SD; n = 3) of Prdm12$^+$ neurons were still TrkA$^+$ and 50.4% ± 4.4% (mean ± SD; n = 3) co-expressed Nav1.8. Only 36.7% ± 6.7% (mean ± SD; n = 4) of Prdm12$^+$ cells co-expressed Runx1, and 32.6% ± 8.3% (mean ± SD; n = 4) of Runx1$^+$ cells did not co-express Prdm12 (Figures 1P–1R), suggesting that Prdm12 is downregulated in some nociceptor subtypes as they mature.

In adult DRGs, we found that 84.6% ± 1.3% (mean ± SD; n = 2) of Prdm12$^+$ neurons were Nav1.8$^+$, 47.8% ± 9.7% (mean ± SD; n = 2) were Runx1$^+$, 31.0% ± 6.3% (mean ± SD; n = 2) were TrkA$^+$, and none co-expressed TrkB or TrkC (Figures 1S–1W). Similar results were obtained in TGs (data not shown). Thus, Prdm12 is selectively expressed in the nociceptive lineage and remains restricted to nociceptors, both peptidergic and non-peptidergic, at the adult stage.

Prdm12 Is Expressed in Both Ngn1- and Ngn2-Expressing Neural Crest-Derived Somatosensory Neural Precursors

In DRG, somatosensory neural precursors go through their final divisions during two broad and overlapping Ngn1- and Ngn2-dependent successive neurogenic waves, each contributing to nociceptors (Lallemend and Ernfors, 2012; Marmigère and Ernfors, 2007). To determine whether *Prdm12* is expressed during

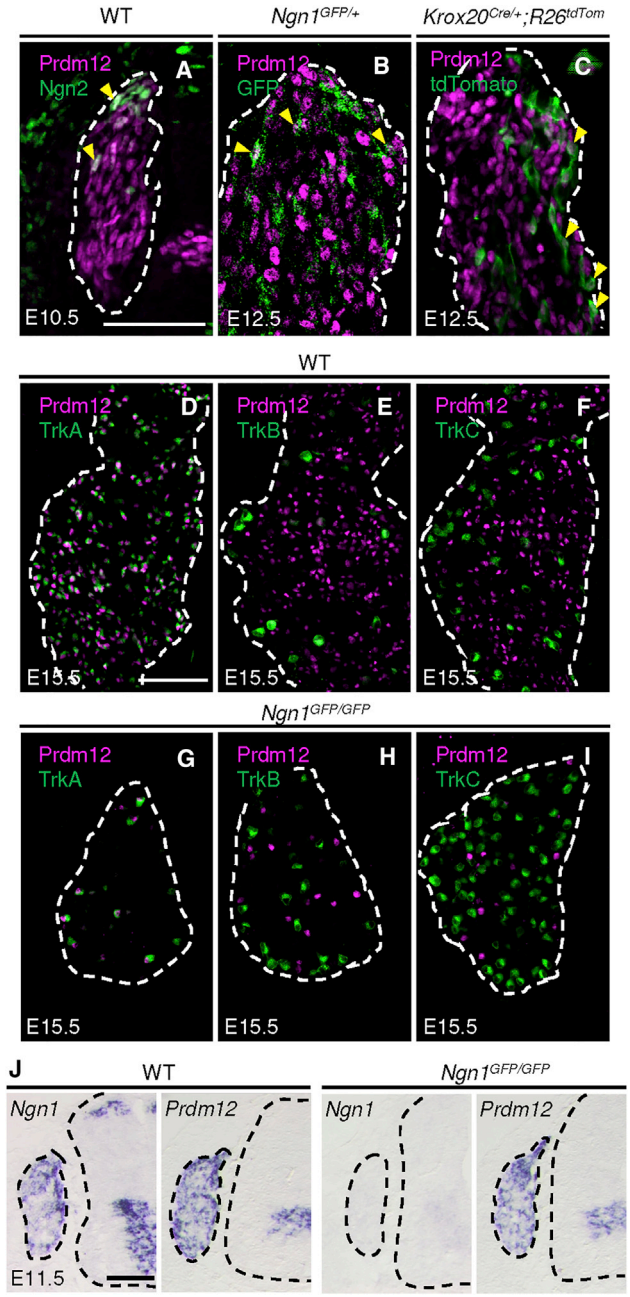

Figure 2. Prdm12 Is Expressed in Precursors of Both Ngn1- and Ngn2-Dependent Neurogenic Waves

Transverse sections of DRG of embryos with the indicated genotype, double immunostained at the indicated stage with Prdm12 (purple) and the indicated markers (green).

(A–C) Comparison of the expression of Prdm12 with that of Ngn2- and Ngn1-expressing cells or with boundary cap-derived cells. Yellow arrowheads point to Prdm12^{+} precursors co-expressing the second analyzed marker (Ngn2 in A, GFP in B, and tdTomato in C).

(D–I) Double immunostaining of Prdm12 and TrkA (D and G), TrkB (E and H), or TrkC (F and I) in DRG of E15.5 WT and *Ngn1*$^{GFP/GFP}$ knockout embryos. Note the severe loss of Prdm12^{+} and TrkA^{+} cells in *Ngn1*$^{GFP/GFP}$ compared to WT and that the few remaining TrkA^{+} cells also express Prdm12 (D and G).

(J) Transverse sections of WT and *Ngn1*$^{GFP/GFP}$ E11.5 embryos hybridized with *Ngn1* or *Prdm12* antisense probes. *Prdm12* expression at that stage appears unaffected by the absence of Ngn1. DRG and spinal cord are delineated with dashed lines. Scale bars, 100 μm.

both phases, we first examined its expression in relation to Ngn2 and Ngn1 expression. Co-expression of Prdm12 with Ngn2^{+} precursors was observed at E9.5 and E10.5 and with Ngn1^{+} precursors or derived differentiating neurons in E12.5 *Ngn1*$^{GFP/+}$ embryos (Figures 2A and 2B) (data not shown). At E12.5, Prdm12 expression was also detected in cells deriving from Krox20^{+} boundary cap (BC) cells that contribute to the second neurogenic wave and generate a subset of nociceptors (Figure 2C; Maro et al., 2004).

We next examined Prdm12 expression in DRG of *Ngn1*$^{GFP/GFP}$ knockout embryos that lack neurons arising from the second neurogenic wave (Ma et al., 1999). TrkA, TrkB, and TrkC were also examined as controls. As expected, at E15.5, many TrkB^{+} and TrkC^{+} neurons were detected in DRG of *Ngn1*$^{GFP/GFP}$ embryos, while TrkA^{+} and Prdm12^{+} cell numbers were dramatically decreased (Figures 2D–2I). The remaining TrkA^{+} neurons observed in *Ngn1*$^{GFP/GFP}$ embryos that likely corresponded to the eTrkA nociceptors generated during the first wave of sensory neurogenesis (Bachy et al., 2011; Lallemend and Ernfors, 2012) all expressed Prdm12. *Prdm12* expression was maintained in the *Ngn1*$^{GFP/GFP}$ embryos at E11.5 (Figure 2J). These results indicate that Prdm12 is expressed in somatosensory precursors arising from the two successive neurogenic waves and suggest that its expression is independent of Ngn1.

Generation of *Prdm12* Constitutive Knockout Embryos

The co-expression of Prdm12 with TrkA suggests that Prdm12 may play a role in nociceptor development. To address this question, we generated *Prdm12* constitutive knockout (KO) mice using a EUCOMM KO-first conditional allele targeting vector allowing expression monitoring (Skarnes et al., 2011). In the targeting construct, an *En2SA-IRES-lacZ* cassette was inserted upstream of exon 2, encoding part of the PRDF1-RIZ (PR) domain, to create a null allele by splicing and premature termination of the transcript (Figure S2A). *Prdm12* exons 2–5 were not detected in qRT-PCR experiments using dissected DRG and spinal cords from *Prdm12*$^{LacZ/LacZ}$ embryos, indicating that the splicing between exon 1 and *En2SA* was effective (Figure S2B). *In situ* hybridization (ISH) and immunofluorescence (IF) experiments using coronal sections of E11.5 *Prdm12*$^{LacZ/LacZ}$ embryos showed no expression of *Prdm12* in DRG and other regions in which it is expressed in the developing nervous system, suggesting that *Prdm12* KO was complete (Figures S2C and S2D). *Prdm12* KO pups died within a few hours of birth. The cause of this lethality remains unclear. Heterozygous *Prdm12*$^{LacZ/+}$ embryos and adult mice displayed no abnormalities compared to wild-type (WT) mice. Whole-mount X-gal staining of E11.5 *Prdm12*$^{LacZ/+}$ embryos showed, as expected, strong staining in the trunk and cranial ganglia, indicating that the inserted gene trap *En2SA-IRES-lacZ* cassette faithfully recapitulates *Prdm12* expression (Figure S2E). These results validate our genetically modified model mice as *Prdm12* constitutive KOs.

Reduced Size of Sensory Ganglia Due to Increased Apoptosis in *Prdm12*$^{LacZ/LacZ}$ Embryos

We first examined whether the genetic deletion of *Prdm12* induced phenotypic abnormalities. At E14.5, whole-mount X-gal staining showed that the TG and DRG of KO embryos were smaller compared to those of *Prdm12*$^{LacZ/+}$ control embryos, and no SJG was detectable (Figure 3A). At E11.5, the reduction in size of the TG and disappearance of the SJG were already detectable in KO embryos, while the DRG appeared normal (Figure S2E). Tlx3 immunostaining of SJGs demonstrated a complete loss of sensory neurons in E13.5 *Prdm12*$^{LacZ/LacZ}$ embryos (Figure 3B). Staining of E13.5 and E14.5 DRG sections with a Peripherin antibody revealed that mutant DRGs contain less neurons and display a selective reduced percentage of small neurons (Figures 3C and 3D).

Examination of Sox10^{+} cells at thoracic levels of E12.5 *Prdm12* KO;*Sox10-Venus* embryos showed that the dorsal and ventral roots of the DRG and the sympathetic ganglia were preserved (Figure S3A). The *Sox10*-Venus reporter mouse line also allowed the indirect visualization of myelinated sensory afferents by the staining of sheathing Schwann cells (Shibata et al., 2010). In accordance with the hypoplasia of DRG observed at E13.5–E14.5, examination of the distal limbs of E14.5 *Prdm12* KO; *Sox10-Venus* revealed a selective loss of small cutaneous sensory fibers, characteristic of lightly myelinated nociceptive afferents (Figure S3B).

The smaller size of sensory ganglia of KO embryos could be due to reduced generation of late sensory neurons or increased cell death. In DRG, immunostaining with an activated caspase-3 antibody revealed increased apoptosis in KO embryos relative to WT controls. This increased rate of apoptosis was detectable starting from E12.5 (Figure 3E). Phospho-histone H3 (pH3) immunostainings were performed at E10.5 and E11.5, indicating that cell proliferation is unaffected in DRG of KO embryos (Figure 3F). Accordingly, the number of Islet1^{+} neurons was equivalent in E11.5 KO and WT embryos (Figure 3G). These results indicate that apoptosis is likely the major cause of the hypoplasia of sensory ganglia in KO embryos. They also suggest that nociceptor development is particularly sensitive to the loss of Prdm12.

Selective Loss of Nociceptor Precursors in Somatosensory Ganglia of *Prdm12* KO Embryos

To test this hypothesis and determine the role of Prdm12 in the generation of the subtypes of somatosensory neurons, we analyzed by ISH the expression of *Ntrk1*, *Ntrk2*, and *Ntrk3* in the DRG of E14.5 KO embryos. We found that *Ntrk1*$^{+}$ nociceptive neurons were absent from the DRG of KO embryos, while the global number of *Ntrk2*$^{+}$ and of *Ntrk3*$^{+}$ neurons appeared comparable to that in WT controls. Immunostainings on E13.5 sections further suggest that the number of TrkB^{+} and TrkC^{+} cells in DRG of KO embryos is similar to that in WT embryos (Figure 3H; Figure S3C). As expected, *Ntrk1* expression was unchanged in the sympathetic ganglia, where *Prdm12* is not expressed (Figure 3I). Similar to DRG, a complete loss of *Ntrk1*$^{+}$ neurons was also observed in TG of E13.5 KO embryos (Figure 3J). Later markers of nociceptors, such as the genes encoding the cold receptor *Trpm8*, the sodium channel Nav1.8 (*Scn10a*), the neurotrophic receptor *Ret*, and the transcription factor *Zbtb20*, which regulates terminal differentiation of nociceptors, were also lost in DRG of E16.5 to postnatal day (P) 0 KO embryos (Figure S3D) (Luo et al., 2007; Peier et al., 2002; Ren et al., 2014). Thus, inactivation of *Prdm12* leads to selective loss of nociceptive precursors by apoptosis.

Prdm12 Is Required for the Initiation of the Expression of the NGF Receptor TrkA in Somatosensory Ganglia

To decipher the molecular mechanisms by which Prdm12 regulates nociceptor development, we carried out a transcriptome analysis by RNA sequencing (RNA-seq) of dissected DRG with the associated spinal cord of E11.5 KO and WT embryos, thus before the onset of apoptosis. Applying a minimal cutoff of $\log_2|0.25|$ fold change and a significance level of false discovery rate (FDR)-adjusted $p < 0.05$, 71 differentially expressed genes were identified in the *Prdm12* KO embryos. Among them, 56 genes were downregulated and 15 genes were upregulated (Figure 4A; Table S1). Gene ontology (GO) analysis of the identified deregulated genes revealed an enrichment in genes involved in neuron specification, as well as sensory neuron and spinal cord development (data not shown). As expected due to the crucial role of Prdm12 in *Xenopus* V1 spinal cord interneuron specification (Thélie et al., 2015), among them were genes involved in the generation of spinal cord V0 (e.g., *Evx1/2*), V1 (e.g., *Foxd3*), and V2 (e.g., *Vsx1* and *Lhx3*) interneurons. As previously reported in the frog, the engrailed-1 (*En1*) V1 marker was lost and the V0 and V2 markers were increased in the spinal cord of KO embryos (Figure S4), suggesting that Prdm12 function in V1 interneuron cell fate specification is conserved in vertebrates. The most highly downregulated gene was *Ntrk1*, whose expression is initiated at E11.5 in DRG (Chen et al., 2006). In addition, general transcriptional regulators of sensory neuron differentiation such as *Neurod1*, *Nhlh1*, and *Brn3a*/*Pou4f1* (Dykes et al., 2011; Ma et al., 1998) were significantly downregulated. Among the few upregulated genes were the transcription factor *Egr2*/*Krox20* expressed in BC cells and its target myelin protein zero (*Mpz*), a marker of Schwann cells (Topilko et al., 1994).

To confirm the differential gene expression revealed by the RNA-seq analysis, we performed ISH of selected deregulated genes on DRG sections of E11.5 embryos. We first examined *Ntrk1*, and among the most downregulated genes were cadherin-related family member 1 (*Cdhr1*), the regulator of G-protein signaling 4 (*Rgs4*), *Tlx2*, *Brn3a*, and *Neurod1*. While in KO embryos *Ntrk1* was abolished, the expression of the other genes tested was only decreased at the edge of the DRG, where new incoming progenitors are mainly located (Marmigère and Ernfors, 2007) (Figure 4B). We next analyzed the upregulated genes *Krox20* and *Mpz* in KO embryos. *Krox20* was expressed ectopically only along the medial edge of the DRG. *Mpz* was also increased, both medially and laterally, suggesting that *Prdm12* may play a role in the maintenance of a somatosensory neural precursor fate, blocking an alternate glial fate, or may affect BC proliferation or migration (Maro et al., 2004) (Figure 4C). We also examined *Ntrk2* and *Ntrk3* that were not differentially regulated in the RNA-seq analysis and found, as expected, that the expression of these markers is comparable in WT and KO embryos (Figure 4D). The disappearance of *Ntrk1* expression in DRG of E11.5 KO, before the loss of TrkA^{+} neurons, provides

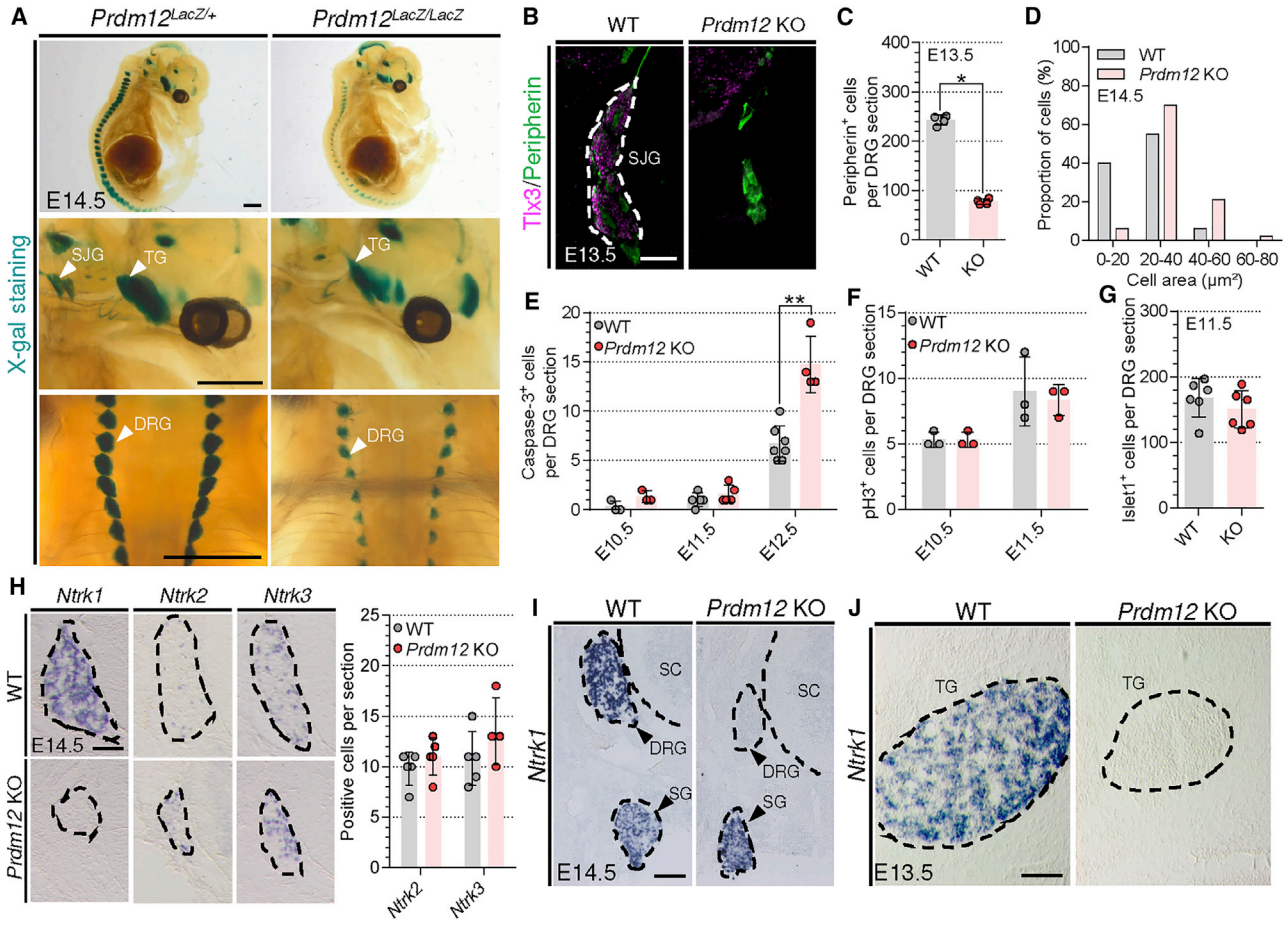

Figure 3. Somatosensory Ganglia Hypoplasia in *Prdm12* KO Embryos Is Due to the Selective Loss of Nociceptors by Apoptosis

(A) Lateral views of X-gal-stained E14.5 control *Prdm12*$^{LacZ/+}$ and *Prdm12*$^{LacZ/LacZ}$ embryos (top). High-magnification views of the head (middle) and dorsal view of the body (bottom) are shown. Note the reduced size of TG and DRG and the loss of SJG (indicated by white arrowheads) in the *Prdm12*$^{LacZ/LacZ}$ embryos. Scale bars, 1,000 μm.

(B) Transverse sections of the SJG of E13.5 wild-type (WT) and *Prdm12* KO embryos double immunostained with antibodies for the pan-neuronal transcription factor Tlx3 and the peripheral nervous system filament protein Peripherin. Scale bar, 100 μm.

(C) DRGs of *Prdm12* KO embryos contain fewer neurons than WT at E13.5. Each dot represents the mean value of Peripherin$^+$ cells in one biological replicate. Mann-Whitney test. *p = 0.029. Mean ± SD.

(D) Histogram of mean soma area of Peripherin$^+$ DRG neurons in E14.5 WT and KO embryos (WT = 1,273 cells; KO = 546 cells; DRG sections from three embryos of each genotype were used).

(E) Increased number of apoptotic cells was observed at E12.5 in *Prdm12* KO embryos. Each dot represents the mean value of caspase-3$^+$ cells in one biological replicate. Mann-Whitney test. E10.5, p = 0.300; E11.5, p = 0.484; E12.5, **p = 0.006. Mean ± SD.

(F) Cell proliferation is unaffected in DRG of E10.5 and E11.5 KO embryos. Each dot represents the mean value of pH3$^+$ cells in one biological replicate. Mann-Whitney test. E10.5, p > 0.999; E11.5, p > 0.999. Mean ± SD.

(G) Neuron number is unchanged in DRG of E11.5 WT and *Prdm12* KO embryos. Each dot represents the mean value of Islet1$^+$ cells in one biological replicate. Mann-Whitney test. p = 0.474. Mean ± SD.

(H) Transverse sections of DRG of E14.5 WT and *Prdm12* KO embryos processed by ISH for *Ntrk1*, *Ntrk2*, and *Ntrk3* (scale bar, 100 μm). The number of *Ntrk2*- and *Ntrk3*-expressing cells appears similar in E14.5 WT and *Prdm12* KO embryos, as estimated by counting their number per section, a method used here so as to take into consideration the reduced size of the DRG in KO embryos. Each dot represents the mean value of positive cells in one biological replicate. Mann-Whitney test. *Ntrk2*, p = 0.191; *Ntrk3*, p = 0.254. Mean ± SD.

(I) ISH on transverse sections of E14.5 WT and KO embryos showing the unaltered expression of *Ntrk1* in sympathetic ganglia. Scale bars, 100 μm.

(J) ISH on transverse sections of the head of E13.5 WT and KO embryos showing that *Ntrk1* is lost in the TG of KO embryos. Scale bar, 100 μm.

TG, trigeminal ganglion; DRG, dorsal root ganglion; SJG, superior-jugular ganglion; SC, spinal cord; SG sympathetic ganglion. SC, DRG, and SG are delineated with dashed lines.

See also Figures S2 and S3.

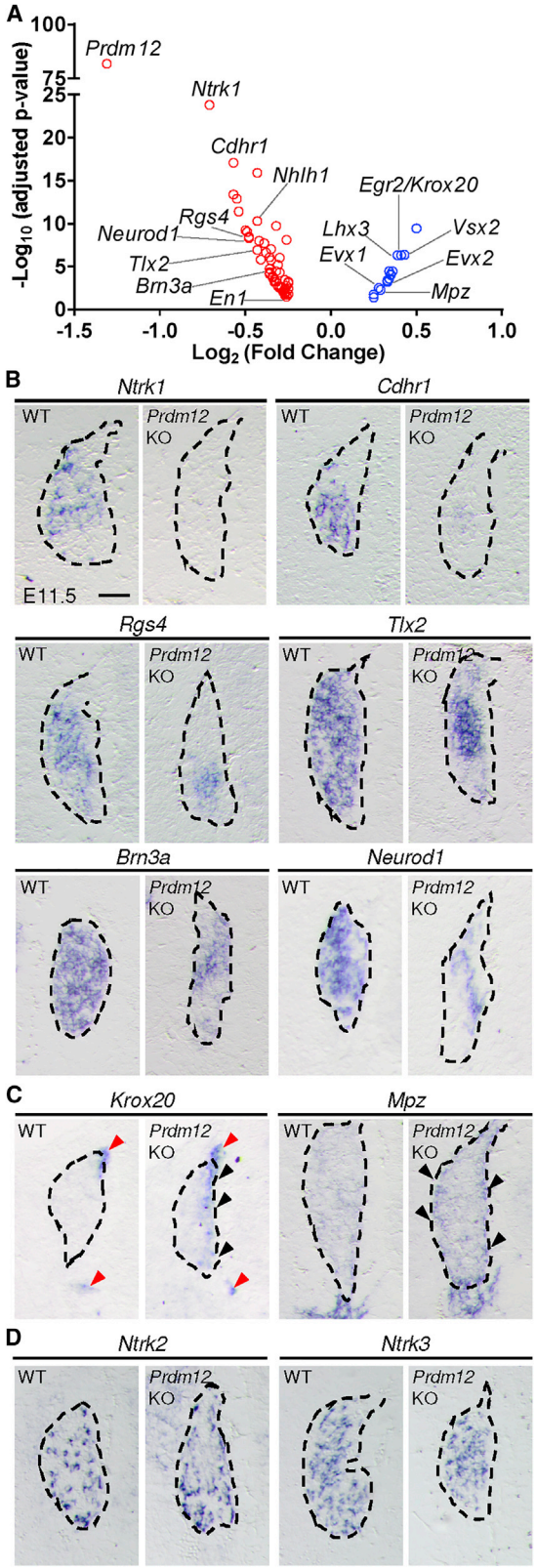

Figure 4. Loss of *Prdm12* Blocks the Initiation of the Expression of *Ntrk1* and Alters the Gene Expression Program of Early Nociceptor Development

(A) Volcano plot showing the fold change and significance of selected misregulated genes in DRG and spinal cord between E11.5 WT versus *Prdm12* KO embryos (four samples per genotype). Downregulated genes are highlighted in red, and upregulated genes are highlighted in blue.

(B–D) ISH analysis of the expression of the indicated genes that are downregulated (B), upregulated (C), or unchanged (D) in the DRG of E11.5 KO embryos compared to WT. Arrowheads in (C) point to ectopic *Krox20* and *Mpz* expression. Dashed lines delineate the DRG. Scale bars, 50 μm.

See also Figure S4 and Table S1.

evidence that loss of *Ntrk1* is likely a direct effect of Prdm12 gene ablation, rather than a secondary effect of cell death. Therefore, *Prdm12* appears to be essential for the initiation of *Ntrk1* expression in somatosensory neural precursors.

Prdm12 Is Required for Postmitotic Nociceptor Maturation and Maintenance of TrkA Expression

To determine whether Prdm12 also plays a role in differentiating postmitotic sensory neurons, we generated *Prdm12* conditional KO (cKO) mice. Mice with floxed exon 2, encoding for most of the PR domain, were generated by crossing $Prdm12^{LacZ/+}$ mice with *ROSA26-Flp* mice (Figure S2A). $Prdm12^{Fl/Fl}$ mice were then crossed with *Advillin*-Cre driver mice expressing the Cre recombinase under the control of the *Advillin* gene promoter, mainly expressed in peripheral sensory neurons (Zhou et al., 2010; Zurborg et al., 2011), to obtain cKO mice.

IF analysis indicate that Prdm12 starts to be efficiently deleted around E14.5 in cKO embryos (Figure 5A), which was confirmed by ISH (Figure S5A). IF and/or ISH analysis of the nociceptive markers Runx1, Nav1.8, the non-peptidergic-specific gene *MrgprD*, *Ntrk1*, *Ret*, *Scn10a*, and the capsaicin-activated heat-sensitive channel transient receptor potential cation channel subfamily V member 1 (TrpV1) (Caterina et al., 1997; Usoskin et al., 2015) in the DRG of E18.5 embryos and/or adult mice revealed that the number of neurons expressing nociceptive markers is markedly reduced in cKO (Figure S5A). We quantified the reduction for Runx1 and TrpV1 and found that their number was reduced by 64.2% ± 18.9% and 70.8% ± 11.5% (mean ± SD; n = 2), respectively, in comparison to controls. Moreover, calcitonin gene-related peptide (CGRP) and isolectin B4 (IB4) immunostainings that reveal peptidergic and non-peptidergic projections, respectively, in the dorsal horn of the spinal cord (Basbaum et al., 2009) were also strongly reduced in adult cKO (Figure S5B). Consistent with the loss of nociceptors, cKO mice displayed an array of injuries mimicking the human *PRDM12* KO phenotype (Figure S5C).

The reduction in expression of nociceptive markers observed at late-embryonic or adult stages in cKO mice may be due to cell death, because the number of $Islet1^+$ neurons in cKO DRG compared to controls gradually decreased and the level of reduction observed at E16.5 was comparable to that of E13.5 KO embryos (Figures 3C and 5A). We therefore examined by IF the expression of TrkA, TrkB, and TrkC from E13.5 to E16.5. While the number of $TrkB^+/TrkC^+$ cells was unchanged, a progressive reduction of $TrkA^+$ cells was detectable in DRG of cKO embryos (Figure 5B). $Ntrk1^+$ staining was also reduced in

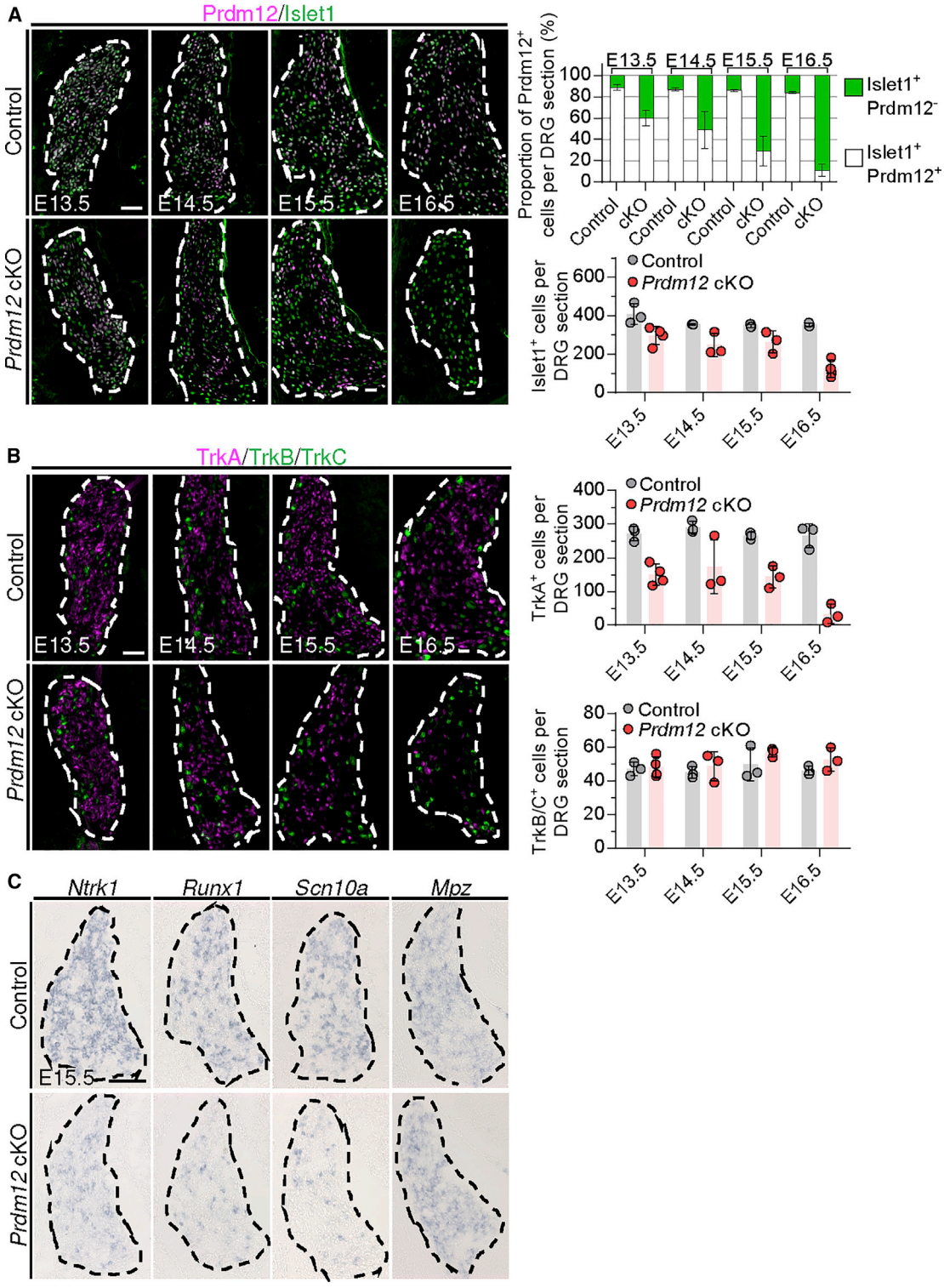

Figure 5. Late Ablation of *Prdm12* in Developing Sensory Neurons Decreases the Expression of *Ntrk1* and Other Nociceptive Markers and Results in a Loss of Nociceptors

Transverse sections of lumbar DRG of *Prdm12* cKO and control embryos immunostained or *in situ* hybridized with the indicated markers.

(A) Proportion of Prdm12$^+$ neurons among Islet1$^+$ neurons in DRG of control and *Prdm12* cKO embryos from E13.5 to E16.5. Islet1$^+$ neurons progressively no longer express Prdm12 (mean ± SD), and their number is gradually reduced (individual values of the biological replicates are indicated with dots).

(legend continued on next page)

SJG and lost in TG of E15.5 cKO embryos (Figure S6). Because *Advillin* expression starts earlier in cranial ganglia (around E11.5) than in DRG (around E12.5) (Hasegawa et al., 2007), and because the TG and SJG are already reduced in size at E14.5 in cKO embryos, downregulation of *Ntrk1* followed by increased cell death must occur earlier in these structures than in DRG.

We next examined by ISH the expression of different nociceptive markers and *Mpz* in DRG of cKO and control embryos at E15.5, when *Prdm12* is efficiently deleted, but before the important cell loss detectable at E16.5. While the expression level of *Ntrk1*, *Runx1*, and *Scn10a* appeared reduced in cKO compared to controls, *Mpz* was unchanged (Figure 5C). Altogether, these results indicate that Prdm12 is required in postmitotic nociceptive neurons for their maturation, which may partly result from its central role in the maintenance of TrkA receptor expression.

Prdm12 Is Regulated by Retinoic Acid in Developing *Xenopus* Trigeminal Placodes and Modulates Ngn1- and Ngn2-Inducing Activity to Promote a Nociceptive Fate

In addition to promoting generic neuronal differentiation, proneural factors function in neuronal subtype specification, activating specific genes and repressing other genes of alternate fates (Bertrand et al., 2002; Guillemot, 2007). Proneural factors often act in conjunction with other factors to drive general and subtype neuronal specification. Prdm8 and Prdm13 have been shown to interact with proneural basic helix-loop-helix (bHLH) transcription factors to repress and modulate their transcriptional activity in the developing cortex and spinal cord, respectively (Chang et al., 2013; Mona et al., 2017; Ross et al., 2012). Because neither Ngn1 nor Ngn2 is able to specify sensory subtypes alone (Zirlinger et al., 2002), we asked whether Ngn1 and Ngn2 function with Prdm12 in somatosensory neuron subtype specification. To approach this question and determine how *Prdm12* is activated in developing cranial sensory ganglia, we turned to the *Xenopus* model that is widely used for investigating neurogenesis. In the *Xenopus* neurula embryo, *Prdm12* is expressed with *Ngn1/2* (Nieber et al., 2009; Thélie et al., 2015) and *Ntrk1/2/3* in developing TG. It is not detected at that stage at the trunk level in primary intramedullar Rohon-Beard sensory neurons but is expressed in extramedullar sensory neurons at later tadpole stages (Figure 6A). We first examined the role of the Ngn1/2 proneural factors and of two other transcription factors that are known to regulate sensory differentiation: Zic1 expressed in the developing anterior neural plate and Pax3, an early marker of the trigeminal placode, in the control of *Prdm12* expression (Adams et al., 2014; Dude et al., 2009; Jaurena et al., 2015; Perron et al., 1999). In gain-of-function experiments in both animal cap (AC) explants and embryos at neurula stage, we found that only Zic1 efficiently induces *Prdm12* (Figures 6B and 6C). Zic1 induces placode formation through its ability to activate retinoic acid (RA) signaling (Jaurena et al., 2015). Accordingly, we found that *Prdm12* upregulation is inhibited by citral, an inhibitor of alcohol and aldehyde dehydrogenases, and activated in trigeminal placodes by low doses of RA, highlighting the important role of RA in *Prdm12* induction in the preplacodal ectoderm (Figures 6D and 6E) (Thélie et al., 2015; Yang and Shinkai, 2013).

Based on these results, we next tested whether *Prdm12* co-expressed with *Ngn1* or *Ngn2* in AC cooperates with these proneural genes to induce *Ntrk1/2/3* and the *TrpV1* nociceptive marker. The spinal cord V1 interneuron marker *En1* was also examined as a positive control for *Prdm12* overexpression (Thélie et al., 2015). Neural β-tubulin (*tubb2b*) expression was monitored to confirm the neuronal fate acquisition of ectodermal explants upon *Ngn1/2* overexpression. As expected, *Ngn1/2* overexpression alone induced to different levels the neuronal markers *Ntrk1/2/3*, *TrpV1*, *En1*, and *Tubb2b*. In contrast, *Prdm12* overexpressed alone was unable to induce any of these markers. When *Prdm12* was co-expressed with *Ngn1*, the induction of *Ntrk1* and *TrpV1* was increased and *Ntrk3* was reduced. When *Prdm12* was co-expressed with *Ngn2*, its ability to induce *Ntrk2* and *Ntrk3* was repressed. While the induction of *Tubb2b* appeared unchanged by the co-expression of *Prdm12*, *En1* was strongly upregulated (Figure 6F).

To determine the contribution of the conserved PR and zinc-finger domains of Prdm12 with Ngn1/2, we tested the activity of a panel of Prdm12 mutants (Yang and Shinkai, 2013). Figure 6G shows that none of them were able to increase the ability of Ngn1 to induce *Ntrk1* or *En1*. Altogether, these data indicate that Prdm12 promotes a nociceptive and V1 interneuron fate at the expense of other cell fates, an activity that requires both its PR and zinc-finger domains. They also suggest that Prdm12 acts in conjunction with proneural factors, modulating their inducing activity.

Prdm12 Promotes a Nociceptor Phenotype in Human Sensory Neurons

In a final set of experiments, we extended the findings of the murine and frog studies to human. We first analyzed PRDM12 expression in DRG of human CS12 embryos. At that stage, some PRDM12$^+$ cells that also express TRKA were observed, indicating that the relationship observed between Prdm12 and TrkA in mouse and frog may be conserved in humans (Figure 7A).

We also assessed the role of PRDM12 in inducing a nociceptor fate in human induced pluripotent stem cells (iPSCs). To generate a *PRDM12*-overexpressing iPSC line (*PRDM12*-RMCE), we performed recombinase-mediated cassette exchange (RMCE) in the Cellectis-FRT line containing an exchangeable cassette in the adeno-associated virus integration site 1 (*AAVS1*) locus (Ordovás et al., 2015) and recombined the cDNA for *PRDM12* under the control of a TET-on promoter. Correct integration of the cassette was validated using junction PCR (data not shown). *PRDM12*-RMCE cells were then fated to anterior neuroectoderm and differentiated into sensory neurons (Figure S7). In the *PRDM12*-RMCE iPSCs cultured without doxycycline induction, we quantified by qRT-PCR the expression of *PRDM12*, *NGN1*, *NGN2*, and *NTRK1* and found that, as expected, their expression is induced upon differentiation into a sensory neuron

(B) TrkA$^+$ neurons are progressively lost in *Prdm12* cKO from E13.5 to E16.5, while no change is detected in the number of TrkB$^+$ and TrkC$^+$ neurons (mean ± SD). Individual values of the biological replicates are indicated with dots.
(C) *Ntrk1*, *Runx1*, *Scn10a*, and *Mpz* expression in E15.5 *Prdm12* cKO and control embryos. Dashed lines delineate the DRG sections. Scale bar, 100 μm.
See also Figures S5 and S6.

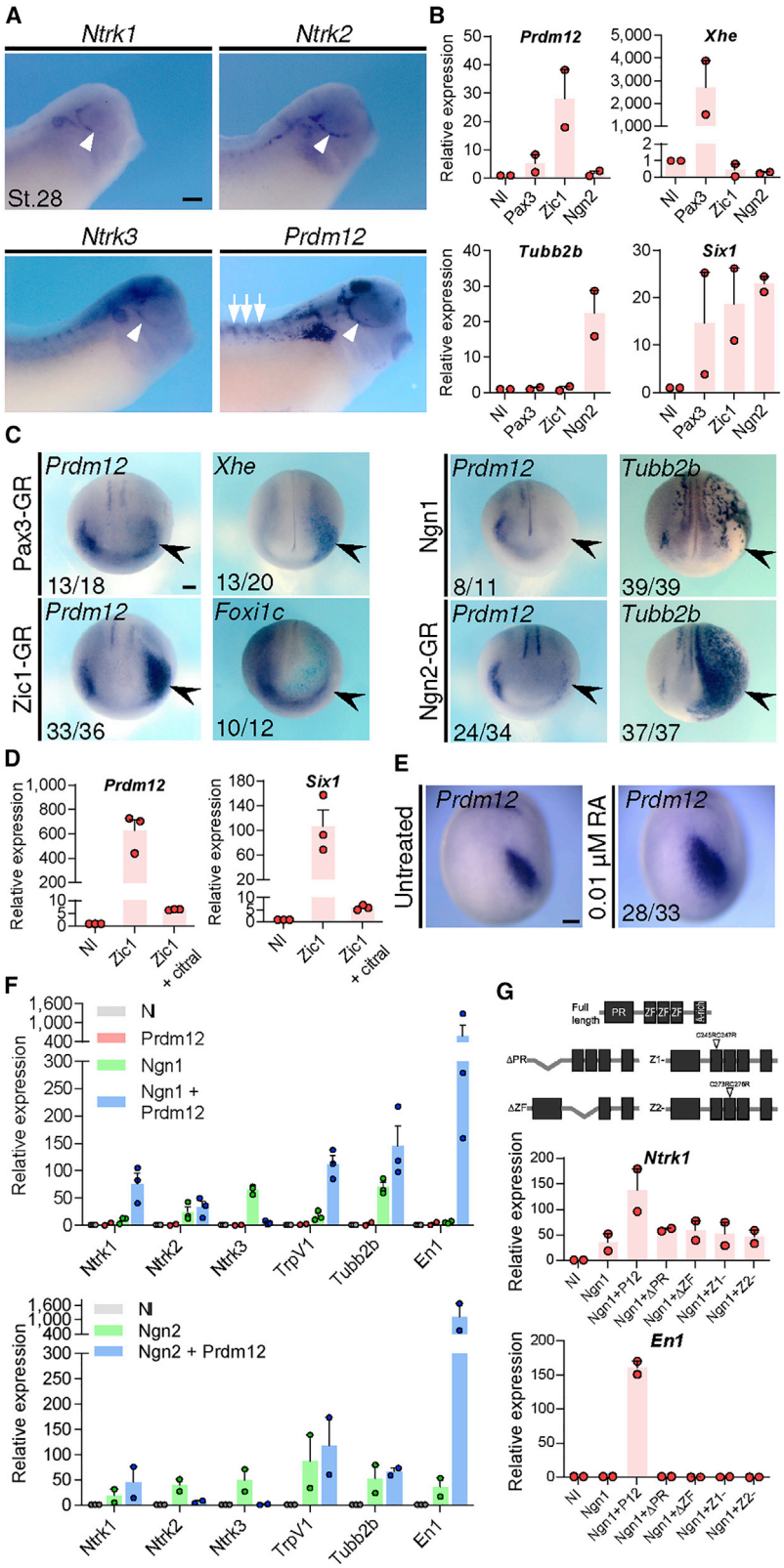

Figure 6. Prdm12 Is Induced by Retinoic Acid and Cooperates with Ngn1 and Ngn2 to Promote a Nociceptor Fate in *Xenopus*

(A) *Prdm12*, *Ntrk1*, *Ntrk2*, and *Ntrk3* are expressed in TG (arrowheads) and DRG (arrows) of stage 28 *Xenopus* tadpoles. Scale bar, 200 μm.

(B) qRT-PCR analysis of *Prdm12* expression in stage 16 AC explants derived from embryos injected with mRNA of *Pax3-GR* (250 pg), *Zic1-GR* (125 pg), or *Ngn2-GR* (250 pg). The hatching gland marker *Xhe*, the pre-placodal marker *Six1*, and the neuronal-specific gene *Tubb2b* were also examined as controls of Pax3-, Zic1-, and Ngn2-inducing activity, respectively.

(C) *Prdm12* expression in *Xenopus* neurula-stage embryos injected unilaterally at the 2-cell stage with *Pax3-GR* (250 pg), *Zic1-GR* (125 pg), *Ngn1* (200 pg), or *Ngn2-GR* (250 pg). *Xhe* that is upregulated by Pax3, *Tubb2b* that is induced by Ngn1/2, and pre-placodal marker *Foxi1c* that is reduced by Zic1 were examined as controls. Arrowheads indicate their altered expression in the trigeminal placode on the injected side revealed by X-gal staining. Scale bar, 200 μm.

(D) Treatment of *Zic1-GR* (125 pg)-overexpressing AC explants with citral (100 μM) blocks *Prdm12* and *Six1* used as controls.

(E) Treatment of intact embryos at stage 11 with RA (0.01 μM) expands *Prdm12*.

(F) qRT-PCR analysis of the expression of the indicated genes in stage 31 animal cap explants overexpressing *Prdm12* (250 pg), *Ngn1* (200 pg), and *Ngn2* (200 pg), alone or in combination, as indicated, showing that Prdm12 modulates the inducing activity of Ngn1/2.

(G) qRT-PCR analysis of *Ntrk1* and *En1* in stage 28 *Xenopus laevis* AC explants derived from embryos co-expressing *Ngn1* and *Prdm12* WT or mutant constructs as indicated, showing that both the PR and the zinc-finger domain of Prdm12 are required for its activity.

In (C) and (E), the total number of injected embryos analyzed and among them those showing the observed phenotype is indicated. In all qRT-PCR experiments, mean ± SEM from at least 2 independent experiments is shown, and the individual values obtained are indicated (red dots).

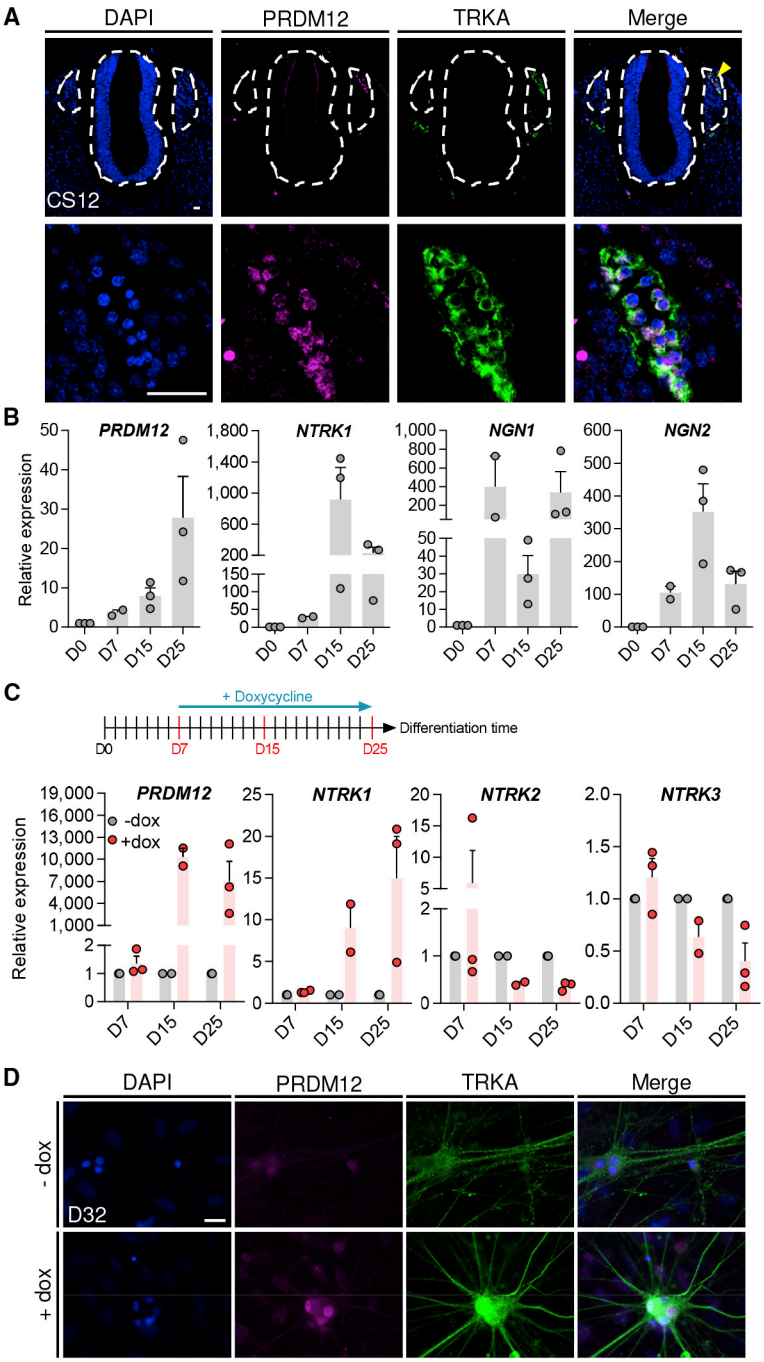

Figure 7. PRDM12 Promotes a Nociceptor Fate in Human Embryonic Stem Cells Differentiated into Sensory Neurons

(A) Transverse sections at the thoracic level of the spinal cord and DRG (delineated with dashed lines) of a CS12 human embryo stained with PRDM12 and TRKA antibodies. Lower panels are high magnifications of some PRDM12$^+$/TRKA$^+$ cells observed in the DRG (indicated by the yellow arrowhead). Scale bars, 25 μm.

(B) qRT-PCR analysis of the expression of *PRDM12*, *NTRK1*, *NGN1*, and *NGN2* in uninduced Prdm12-RMCE iPSCs differentiated into sensory neurons and harvested at day 7, 15, or 25 of differentiation. Expression levels were compared to the level in undifferentiated iPSCs, defined as 1 (mean ± SEM).

(C) qRT-PCR analysis of the expression of *PRDM12*, *NTRK1*, *NTRK2*, and *NTRK3* in doxycycline-induced Prdm12-RMCE iPSCs differentiated into sensory neurons and harvested until day 7, 15, or 25 of differentiation. Expression levels were compared to the expression level in uninduced control cells, which was defined as 1 (mean ± SEM).

(D) Immunostaining of TRKA and PRDM12 on Prdm12-RMCE iPSCs differentiated into sensory neurons and harvested at day 32. Scale bar, 25 μm. See also Figure S7.

In (B) and (C), individual values for biological replicates are indicated (dots).

phenotype (Figure 7B). To induce expression of *PRDM12*, doxycycline was added from day 7 until day 25 of differentiation. Consistent with the *Xenopus* AC assays, qRT-PCR analysis of doxycycline-treated and untreated cells on days 7, 15, and 25 demonstrated that overexpression of *PRDM12* increases *NTRK1* but decreases *NTRK2* and *NTRK3* (Figure 7C). The increased level of TrkA expression in *Prdm12*-overexpressing cells compared to controls was also evident by immunostaining (Figure 7D). These results indicated that as in mouse and *Xenopus*, Prdm12 promotes a nociceptor phenotype in human sensory neurons.

DISCUSSION

All nociceptors require TrkA (*Ntrk1*) and its major ligand NGF for their survival and maturation during development, but little is known about the mechanisms that drive *Ntrk1* expression in DRG neuronal precursors. Using constitutive and conditional *Prdm12* KO mouse models and gain-of-function approaches in *Xenopus* and human iPSCs, we provide evidence that Prdm12, acting in conjunction with Neurogenin proneural factors, plays an essential role in the emergence of nociceptors in sensory ganglia partly through the regulation of the initiation and maintenance of *Ntrk1* expression, allowing their survival and differentiation during development.

Several transcription factors have been identified that contribute to the regulation of TrkA expression in nociceptors. Among them are Brn3a, Klf7, and Runx1 (Huang et al., 1999; Lei et al., 2005, 2006; Marmigère et al., 2006). Brn3a and Klf7 are expressed in most, if not all, DRG and TG sensory neurons, while Prdm12 and Runx1 are restricted to TrkA$^+$ neurons, with *Prdm12* preceding and *Runx1* following the onset of TrkA expression at E11.5. In TG of *Brn3a* mutant mice, Brn3a is required for TrkC expression, as well as for the maintenance, but not the initiation, of TrkA and TrkB expression, and Brn3a loss results in sensory neuron death (Huang et al., 1999). In DRG of *Brn3a* KO embryos, neurons are apparently not lost but present broad specification and axonal projection defects (Xiang et al., 1996; Zou et al., 2012). The ablation of *Klf7* leads

to a specific reduction of TrkA$^+$ neurons, as observed in *Prdm12* KO embryos. However, expression of TrkA in sensory ganglia of E11.5 *Klf7* mutants is normal, indicating that *Klf7* is dispensable for the initiation of TrkA receptor expression (Lallemend and Ernfors, 2012; Lei et al., 2006; Marmigère and Ernfors, 2007). Finally, Runx1 mainly acts during late sensory neurogenesis as a repressor of *Ntrk1* (Luo et al., 2007). Prdm12 is thus the first transcriptional regulator identified whose expression is restricted to developing nociceptors and is required for the initiation and maintenance of *Ntrk1* expression.

What are the Prdm12 target genes in developing nociceptors? We here show that at E11.5, Prdm12 appears to contribute to the regulation of the expression of several other nociceptive genes aside from *Ntrk1* in neural or neuronal precursors. Before the wave of apoptosis caused by loss of *Prdm12*, genes encoding early sensory transcription factors such as *Nhlh1*, *Brn3a*, and *Neurod1* were significantly downregulated in KO DRG. *Runx1* may also be under the control of Prdm12, because its expression was undetectable at E12.5 in KO embryos (data not shown) and was decreased in cKO at E15.5. *Krox20*, which labels BC cells that participate in the second wave of sensory neurogenesis and was found to be ectopically expressed in DRG of E11.5 KO embryos, may be another Prdm12 target. Ectopic Krox20$^+$ cells have been also described in the DRGs of DBZEB transgenic mice that exhibit a reduced number of nociceptors. This increase reflects the developmental plasticity of the somatosensory system and the participation of BC cells to a compensatory mechanism ensuring the formation of sufficient nociceptive neurons (Ohayon et al., 2015), which may also be the case in the DRG of *Prdm12* KO mice. However, no rescue was observed in our KO, and *Mpz* was increased. This suggests that BC cells need Prdm12 to differentiate into nociceptors and that in the absence of Prdm12, BC-derived cells may have adopted an alternate glial fate. Ectopic expression of *Krox20* was undetectable in the DRG of *Prdm12* KO mice at E14.5 (data not shown), suggesting that those cells may have finally also undergone apoptosis.

In contrast to null mutants, we did not observe an upregulation of *Mpz* in the DRG of cKO embryos, indicating that the loss of Prdm12 is not sufficient to switch the fate of postmitotic differentiating nociceptors to glia. Although it is likely that the decrease of the expression of many nociceptive markers observed in the DRG of E18.5 cKO embryos is due to cell loss, our results suggest that Prdm12 plays a role in the regulation of several ion channels and receptors. A decrease in their expression was already detectable in cKO embryos at E15.5, when the loss of Prdm12 in DRG appears to be completed and the number of DRG neurons in cKO and control embryos is still almost similar. An important example of this is *Scn10a*, a gene encoding the voltage-gated sodium channel Nav1.8 essential for the generation of action potentials in nociceptors (Faber et al., 2012). Altogether, our data indicate that Prdm12 plays an essential role in nociceptor specification and that it functions in postmitotic nociceptors, perhaps as a terminal selector gene, controlling late steps of their differentiation, as has been described in worms (Masoudi et al., 2018).

How does Prdm12 specify nociceptors and regulate its targets? Although we did not observe an increase in *Ntrk2/3*-positive neurons in DRG of *Prdm12* KO and cKO mutants, *Prdm12* gain of function was shown to induce *Ntrk1* and reduce *Ntrk2/3*. These data suggest that Prdm12 may specify the TrkA lineage not only by promoting, directly or indirectly, *Ntrk1* activation but also by inhibiting the expression of *Ntrk2/3*. Loss of *Ntrk1* in DRG of *Prdm12* KO and cKO embryos is not compensated by an increase in *Ntrk2/3*-positive neurons, likely because the absence of Prdm12 is not sufficient to upregulate the expression of transcription factors such as Runx3 and Shox2 that are required for their expression (Lallemend and Ernfors, 2012). In the developing spinal cord, Prdm12 controls V1 interneuron formation by acting as a repressor for genes encoding determinants of alternate V0 and V2 fates (Thélie et al., 2015). In the DRG, however, our transcriptomic analysis did not reveal any overexpressed gene that could account for the full repression of *Ntrk1* observed in *Prdm12* KO DRG. The identification of *Prdm12* direct transcriptional targets in the developing DRG will thus be a crucial step to better understand its mechanism of action and determine whether it acts in this context as a repressor, an activator, or both, as is the case for other PRDM factors (Hohenauer and Moore, 2012).

The nature of the partners in the Prdm12 transcriptional complex is another important question. Prdm12 is thought to bind indirectly to DNA via other transcription factors (Thélie et al., 2015) whose identity is unknown. In somatosensory neural precursors, our data suggest that Prdm12 promotes a nociceptive fate by modulating the inducing activity of the bHLH proteins Ngn1/2. Ngn1 and Ngn2 are also likely Prdm12 partners in the spinal cord, because they are co-expressed in p1 progenitors and the co-expression of Ngn1/2 with Prdm12 leads to a dramatic synergistic upregulation of the V1 marker En1. Whether Prdm12 physically interacts with proneural factors, as do other members of the family (Chang et al., 2013; Mona et al., 2017; Ross et al., 2012), is not clear. Using the Bimolecular fluorescence complementation (BiFC) assay approach (Saka et al., 2007), overexpressing in ACs Prdm12 fused to the C terminus of Venus yellow fluorescent protein (YFP) alone or with Ngn1 or Ngn2 fused to the N terminus of Venus YFP, we have observed that the co-expression of Prdm12 with Ngn1, but not Ngn2, gives rise to a clear nuclear fluorescent signal, as observed when Ngn1 is overexpressed with its partner E12 (data not shown), suggesting that Prdm12 may physically interact with some proneural factors. Prdm12 lacks intrinsic histone methyltransferase activity and recruits G9a (Ehmt2) to dimethylate histone H3 at lysine 9 (Yang and Shinkai, 2013). Hence, Prdm12 overexpression robustly increases histone H3 lysine 9 dimethylation (H3K9me2) in *Xenopus* embryos (Chen et al., 2015). G9a is expressed in nociceptors, where it regulates the expression of many genes, including K$^+$ channels (Laumet et al., 2015). Whether Prdm12 acts by recruiting the co-repressor G9a or other co-factors to epigenetically regulate gene expression in developing nociceptors remains to be investigated.

The putative upstream genes and signals controlling *Prdm12* expression in developing sensory ganglia largely remain to be addressed. Here we show that in frog cranial ganglia, *Prdm12* is activated by RA and by the transcription factor Zic1, which induces placode formation non-cell autonomously

through its ability to induce RA production (Jaurena et al., 2015), but not by Ngn1/2 overexpression. In accordance with these observations, we found that in mouse DRG, *Prdm12* expression is independent of Ngn1. This is in contrast to Runx1, which is not detected at E14.5 in *Ngn1* mutants (Kramer et al., 2006). The close association of Prdm12 and TrkA expression raises the question of whether Prdm12, which is essential for TrkA initiation, is in turn regulated by the NGF-TrkA signaling.

In adult mice and humans, NGF signaling induces nociceptor sensitization, leading to chronic pain states (Denk et al., 2017). Pharmacotherapies targeting this pathway appear to be a promising strategy in the treatment of chronic pain conditions. The importance of epigenetic mechanisms in the induction and maintenance of chronic pain (Denk and McMahon, 2012; Laumet et al., 2015) and the persistent highly restricted expression of Prdm12 in mature nociceptors suggest that it is a promising target for the development of novel methods for pain relief.

STAR★METHODS

Detailed methods are provided in the online version of this paper and include the following:

- KEY RESOURCES TABLE
- CONTACT FOR REAGENT AND RESOURCE SHARING
- EXPERIMENTAL MODEL AND SUBJECT DETAILS
  - Mice
  - Frogs
  - PRDM12-RMCE cell line
  - Human embryonic samples
- METHOD DETAILS
  - ISHs and immunostainings
  - Rabbit and guinea pig anti-PRDM12 antibodies
  - Whole-mount X-gal staining of embryos
  - *Xenopus* embryo microinjections and AC assays
  - Differentiation of human pluripotent stem cells to nociceptors
  - Real-time RT-qPCR
  - Human embryo immunostainings
  - RNA sequencing and data processing
- QUANTIFICATION AND STATISTICAL ANALYSIS
  - Statistical analysis
  - Replications
  - Randomization
- DATA AND SOFTWARE AVAILABILITY

SUPPLEMENTAL INFORMATION

Supplemental Information can be found with this article online at https://doi.org/10.1016/j.celrep.2019.02.097.

ACKNOWLEDGMENTS

We thank T. Lingner, O. Shomroni, and K. Raithatha for the RNA-seq analysis; A. Souza, K. Eggermont, S. Noens, and M. Geraerts for the optimization of the sensory neuron differentiation protocol; A. Souza and M. Welters for the generation of the *PRDM12*-RMCE line; and R. Heinen for the generation of the His tagged-*Prdm12* construct used to generate the protein for Prdm12 antibody production. We acknowledge F. Clotman, T.M. Jessell, Q. Ma, A. Pattyn, J.M. Penninger, L.F. Reichardt, and P. Topilko for providing reagents or embryos; members of the Centre for Microscopy and Molecular Imaging (CMMI) for help with imaging techniques; and J.C. Marine for editing the manuscript. This work was supported by grants from the FNRS (CDR 29148846), the Walloon Region (First International project EPIGENE 121784), the Association Belge contre les Maladies Neuro-Musculaires, the Belgian Pain Society, the Rotary and the Fondation de France (to E.J.B.), IWT SBO iPS-CAF-150031 and KU-Leuven IOFM-13-0227-KULSTEM, and C14/17/111-3D-MUSIC funding (to C.V.), and the NHS-NIHR Cambridge Biomedical Research Centre (to C.G.W.). S.D. and S.V. are FRIA doctoral fellows, and C.V.C. an FNRS postdoctoral fellow.

AUTHOR CONTRIBUTIONS

C.V.C. and V.N. contributed to the generation of the *Prdm12* KO and cKO mice. S.D. and S.V. performed the Prdm12 expression analysis and the characterization of the phenotype of the KO and cKO embryos and the frog experiments, with the help of S.K. E.V.F. performed the PRDM12 immunostaining on human embryo sections. E.M. and T.V. performed the experiments in iPSCs. S.R. performed the BiFC analysis. C.V.C., S.D., S.V., E.M., S.R., E.V.F., B.Z.S., K.A.H., T.P., C.G.W., V.N., C.V., and E.J.B. analyzed the data. E.J.B., C.V., and V.N. conceived and supervised the project. S.D., S.V., and E.J.B. wrote the manuscript.

DECLARATION OF INTERESTS

The authors declare no competing interests.

Received: October 15, 2018
Revised: January 21, 2019
Accepted: February 25, 2019
Published: March 26, 2019

REFERENCES

Adams, J.S., Sudweeks, S.N., and Stark, M.R. (2014). Pax3 isoforms in sensory neurogenesis: expression and function in the ophthalmic trigeminal placode. Dev. Dyn. *243*, 1249–1261.

Anders, S., and Huber, W. (2010). Differential expression analysis for sequence count data. Genome Biol. *11*, R106.

Bachy, I., Franck, M.C.M., Li, L., Abdo, H., Pattyn, A., and Ernfors, P. (2011). The transcription factor Cux2 marks development of an A-delta sublineage of TrkA sensory neurons. Dev. Biol. *360*, 77–86.

Barlow, L.A. (2002). Cranial nerve development: placodal neurons ride the crest. Curr. Biol. *12*, R171–R173.

Basbaum, A.I., Bautista, D.M., Scherrer, G., and Julius, D. (2009). Cellular and molecular mechanisms of pain. Cell *139*, 267–284.

Bertrand, N., Castro, D.S., and Guillemot, F. (2002). Proneural genes and the specification of neural cell types. Nat. Rev. Neurosci. *3*, 517–530.

Bindea, G., Mlecnik, B., Hackl, H., Charoentong, P., Tosolini, M., Kirilovsky, A., Fridman, W.H., Pagès, F., Trajanoski, Z., and Galon, J. (2009). ClueGO: a Cytoscape plug-in to decipher functionally grouped gene ontology and pathway annotation networks. Bioinformatics *25*, 1091–1093.

Bullen, P., and Wilson, D. (1997). The Carnegie Staging of Human Embryos: a Practical Guide. In Molecular Genetics of Early Human Development, T. Strachan, S. Lindsay, and D. Wilson, eds. (Bios Scientific Publishers), pp. 27–35.

Caterina, M.J., Schumacher, M.A., Tominaga, M., Rosen, T.A., Levine, J.D., and Julius, D. (1997). The capsaicin receptor: a heat-activated ion channel in the pain pathway. Nature *389*, 816–824.

Cau, E., Gradwohl, G., Fode, C., and Guillemot, F. (1997). Mash1 activates a cascade of bHLH regulators in olfactory neuron progenitors. Development *124*, 1611–1621.

Chambers, S.M., Qi, Y., Mica, Y., Lee, G., Zhang, X.J., Niu, L., Bilsland, J., Cao, L., Stevens, E., Whiting, P., et al. (2012). Combined small-molecule inhibition accelerates developmental timing and converts human pluripotent stem cells into nociceptors. Nat. Biotechnol. *30*, 715–720.

Chang, J.C., Meredith, D.M., Mayer, P.R., Borromeo, M.D., Lai, H.C., Ou, Y.H., and Johnson, J.E. (2013). Prdm13 mediates the balance of inhibitory and excitatory neurons in somatosensory circuits. Dev. Cell *25*, 182–195.

Chen, C.L., Broom, D.C., Liu, Y., de Nooij, J.C., Li, Z., Cen, C., Samad, O.A., Jessell, T.M., Woolf, C.J., and Ma, Q. (2006). Runx1 determines nociceptive sensory neuron phenotype and is required for thermal and neuropathic pain. Neuron *49*, 365–377.

Chen, Y.C., Auer-Grumbach, M., Matsukawa, S., Zitzelsberger, M., Themistocleous, A.C., Strom, T.M., Samara, C., Moore, A.W., Cho, L.T., Young, G.T., et al. (2015). Transcriptional regulator PRDM12 is essential for human pain perception. Nat. Genet. *47*, 803–808.

Denk, F., and McMahon, S.B. (2012). Chronic pain: emerging evidence for the involvement of epigenetics. Neuron *73*, 435–444.

Denk, F., Bennett, D.L., and McMahon, S.B. (2017). Nerve Growth Factor and Pain Mechanisms. Annu. Rev. Neurosci. *40*, 307–325.

Dobin, A., Davis, C.A., Schlesinger, F., Drenkow, J., Zaleski, C., Jha, S., Batut, P., Chaisson, M., and Gingeras, T.R. (2013). STAR: ultrafast universal RNA-seq aligner. Bioinformatics *29*, 15–21.

Dude, C.M., Kuan, C.Y.K., Bradshaw, J.R., Greene, N.D.E., Relaix, F., Stark, M.R., and Baker, C.V.H. (2009). Activation of Pax3 target genes is necessary but not sufficient for neurogenesis in the ophthalmic trigeminal placode. Dev. Biol. *326*, 314–326.

Dykes, I.M., Tempest, L., Lee, S.-I., and Turner, E.E. (2011). Brn3a and Islet1 act epistatically to regulate the gene expression program of sensory differentiation. J. Neurosci. *31*, 9789–9799.

Faber, C.G., Lauria, G., Merkies, I.S.J., Cheng, X., Han, C., Ahn, H.-S., Persson, A.-K., Hoeijmakers, J.G.J., Gerrits, M.M., Pierro, T., et al. (2012). Gain-of-function Nav1.8 mutations in painful neuropathy. Proc. Natl. Acad. Sci. USA *109*, 19444–19449.

Faber, J., and Nieuwkoop, P.D. (1994). Normal Table of *Xenopus laevis* (Daudin): A Systematical & Chronological Survey of the Development from the Fertilized Egg till the End of Metamorphosis (Garland Science).

Fog, C.K., Galli, G.G., and Lund, A.H. (2012). PRDM proteins: important players in differentiation and disease. BioEssays *34*, 50–60.

Gerrelli, D., Lisgo, S., Copp, A.J., and Lindsay, S. (2015). Enabling research with human embryonic and fetal tissue resources. Development *142*, 3073–3076.

Guillemot, F. (2007). Spatial and temporal specification of neural fates by transcription factor codes. Development *134*, 3771–3780.

Hanotel, J., Bessodes, N., Thélie, A., Hedderich, M., Parain, K., Van Driessche, B., Brandão, Kde.O., Kricha, S., Jorgensen, M.C., Grapin-Botton, A., et al. (2014). The Prdm13 histone methyltransferase encoding gene is a Ptf1a-Rbpj downstream target that suppresses glutamatergic and promotes GABAergic neuronal fate in the dorsal neural tube. Dev. Biol. *386*, 340–357.

Harrington, A.W., and Ginty, D.D. (2013). Long-distance retrograde neurotrophic factor signalling in neurons. Nat. Rev. Neurosci. *14*, 177–187.

Hasegawa, H., Abbott, S., Han, B.-X., Qi, Y., and Wang, F. (2007). Analyzing somatosensory axon projections with the sensory neuron-specific Advillin gene. J. Neurosci. *27*, 14404–14414.

Hatano, M., Iitsuka, Y., Yamamoto, H., Dezawa, M., Yusa, S., Kohno, Y., and Tokuhisa, T. (1997). Ncx, a Hox11 related gene, is expressed in a variety of tissues derived from neural crest cells. Anat. Embryol. (Berl.) *195*, 419–425.

Hoekstra, E.J., von Oerthel, L., van der Linden, A.J.A., Schellevis, R.D., Scheppink, G., Holstege, F.C.P., Groot-Koerkamp, M.J., van der Heide, L.P., and Smidt, M.P. (2013). Lmx1a is an activator of Rgs4 and Grb10 and is responsible for the correct specification of rostral and medial mdDA neurons. Eur. J. Neurosci. *37*, 23–32.

Hohenauer, T., and Moore, A.W. (2012). The Prdm family: expanding roles in stem cells and development. Development *139*, 2267–2282.

Hong, C.-S., and Saint-Jeannet, J.-P. (2007). The activity of Pax3 and Zic1 regulates three distinct cell fates at the neural plate border. Mol. Biol. Cell *18*, 2192–2202.

Huang, E.J., Zang, K., Schmidt, A., Saulys, A., Xiang, M., and Reichardt, L.F. (1999). POU domain factor Brn-3a controls the differentiation and survival of trigeminal neurons by regulating Trk receptor expression. Development *126*, 2869–2882.

Jaurena, M.B., Juraver-Geslin, H., Devotta, A., and Saint-Jeannet, J.P. (2015). Zic1 controls placode progenitor formation non-cell autonomously by regulating retinoic acid production and transport. Nat. Commun. *6*, 7476.

Joyner, A.L., and Martin, G.R. (1987). En-1 and En-2, two mouse genes with sequence homology to the *Drosophila* engrailed gene: expression during embryogenesis. Genes Dev. *1*, 29–38.

Kinameri, E., Inoue, T., Aruga, J., Imayoshi, I., Kageyama, R., Shimogori, T., and Moore, A.W. (2008). Prdm proto-oncogene transcription factor family expression and interaction with the Notch-Hes pathway in mouse neurogenesis. PLoS ONE *3*, e3859.

Kramer, I., Sigrist, M., de Nooij, J.C., Taniuchi, I., Jessell, T.M., and Arber, S. (2006). A role for Runx transcription factor signaling in dorsal root ganglion sensory neuron diversification. Neuron *49*, 379–393.

Lallemend, F., and Ernfors, P. (2012). Molecular interactions underlying the specification of sensory neurons. Trends Neurosci. *35*, 373–381.

Laumet, G., Garriga, J., Chen, S.R., Zhang, Y., Li, D.P., Smith, T.M., Dong, Y., Jelinek, J., Cesaroni, M., Issa, J.P., and Pan, H.L. (2015). G9a is essential for epigenetic silencing of K(+) channel genes in acute-to-chronic pain transition. Nat. Neurosci. *18*, 1746–1755.

Lei, L., Laub, F., Lush, M., Romero, M., Zhou, J., Luikart, B., Klesse, L., Ramirez, F., and Parada, L.F. (2005). The zinc finger transcription factor Klf7 is required for TrkA gene expression and development of nociceptive sensory neurons. Genes Dev. *19*, 1354–1364.

Lei, L., Zhou, J., Lin, L., and Parada, L.F. (2006). Brn3a and Klf7 cooperate to control TrkA expression in sensory neurons. Dev. Biol. *300*, 758–769.

Li, H., Handsaker, B., Wysoker, A., Fennell, T., Ruan, J., Homer, N., Marth, G., Abecasis, G., and Durbin, R.; 1000 Genome Project Data Processing Subgroup (2009). The Sequence Alignment/Map format and SAMtools. Bioinformatics *25*, 2078–2079.

Luo, W., Wickramasinghe, S.R., Savitt, J.M., Griffin, J.W., Dawson, T.M., and Ginty, D.D. (2007). A hierarchical NGF signaling cascade controls Ret-dependent and Ret-independent events during development of nonpeptidergic DRG neurons. Neuron *54*, 739–754.

Ma, Q., Chen, Z., del Barco Barrantes, I., de la Pompa, J.L., and Anderson, D.J. (1998). neurogenin1 is essential for the determination of neuronal precursors for proximal cranial sensory ganglia. Neuron *20*, 469–482.

Ma, Q., Fode, C., Guillemot, F., and Anderson, D.J. (1999). Neurogenin1 and neurogenin2 control two distinct waves of neurogenesis in developing dorsal root ganglia. Genes Dev. *13*, 1717–1728.

Marmigère, F., and Ernfors, P. (2007). Specification and connectivity of neuronal subtypes in the sensory lineage. Nat. Rev. Neurosci. *8*, 114–127.

Marmigère, F., Montelius, A., Wegner, M., Groner, Y., Reichardt, L.F., and Ernfors, P. (2006). The Runx1/AML1 transcription factor selectively regulates development and survival of TrkA nociceptive sensory neurons. Nat. Neurosci. *9*, 180–187.

Maro, G.S., Vermeren, M., Voiculescu, O., Melton, L., Cohen, J., Charnay, P., and Topilko, P. (2004). Neural crest boundary cap cells constitute a source of neuronal and glial cells of the PNS. Nat. Neurosci. *7*, 930–938.

Masoudi, N., Tavazoie, S., Glenwinkel, L., Ryu, L., Kim, K., and Hobert, O. (2018). Unconventional function of an Achaete-Scute homolog as a terminal selector of nociceptive neuron identity. PLoS Biol. *16*, e2004979.

Mattar, P., Langevin, L.M., Markham, K., Klenin, N., Shivji, S., Zinyk, D., and Schuurmans, C. (2008). Basic helix-loop-helix transcription factors cooperate to specify a cortical projection neuron identity. Mol. Cell. Biol. *28*, 1456–1469.

Mona, B., Uruena, A., Kollipara, R.K., Ma, Z., Borromeo, M.D., Chang, J.C., and Johnson, J.E. (2017). Repression by PRDM13 is critical for generating precision in neuronal identity. eLife *6*, 1–26.

Mzoughi, S., Tan, Y.X., Low, D., and Guccione, E. (2016). The role of PRDMs in cancer: one family, two sides. Curr. Opin. Genet. Dev. *36*, 83–91.

Nagy, V., Cole, T., Van Campenhout, C., Khoung, T.M., Leung, C., Vermeiren, S., Novatchkova, M., Wenzel, D., Cikes, D., Polyansky, A.A., et al. (2015). The evolutionarily conserved transcription factor PRDM12 controls sensory neuron development and pain perception. Cell Cycle *14*, 1799–808.

Nahorski, M.S., Chen, Y.C., and Woods, C.G. (2015). New Mendelian Disorders of Painlessness. Trends Neurosci. *38*, 712–724.

Nieber, F., Pieler, T., and Henningfeld, K.A. (2009). Comparative expression analysis of the neurogenins in *Xenopus tropicalis* and *Xenopus laevis*. Dev. Dyn. *238*, 451–458.

Ohayon, D., Ventéo, S., Sonrier, C., Lafon, P.-A., Garcès, A., Valmier, J., Rivat, C., Topilko, P., Carroll, P., and Pattyn, A. (2015). Zeb family members and boundary cap cells underlie developmental plasticity of sensory nociceptive neurons. Dev. Cell *33*, 343–350.

Ordovás, L., Boon, R., Pistoni, M., Chen, Y., Wolfs, E., Guo, W., Sambathkumar, R., Bobis-Wozowicz, S., Helsen, N., Vanhove, J., et al. (2015). Efficient Recombinase-Mediated Cassette Exchange in hPSCs to Study the Hepatocyte Lineage Reveals AAVS1 Locus-Mediated Transgene Inhibition. Stem Cell Reports *5*, 918–931.

Oschwald, R., Richter, K., and Grunz, H. (1991). Localization of a nervous system-specific class II β-tubulin gene in *Xenopus laevis* embryos by whole-mount *in situ* hybridization. Int. J. Dev. Biol. *35*, 399–405.

Peier, A.M., Moqrich, A., Hergarden, A.C., Reeve, A.J., Andersson, D.A., Story, G.M., Earley, T.J., Dragoni, I., McIntyre, P., Bevan, S., and Patapoutian, A. (2002). A TRP channel that senses cold stimuli and menthol. Cell *108*, 705–715.

Perron, M., Opdecamp, K., Butler, K., Harris, W.A., and Bellefroid, E.J. (1999). X-ngnr-1 and Xath3 promote ectopic expression of sensory neuron markers in the neurula ectoderm and have distinct inducing properties in the retina. Proc. Natl. Acad. Sci. USA *96*, 14996–15001.

Qi, L., Huang, C., Wu, X., Tao, Y., Yan, J., Shi, T., Cao, C., Han, L., Qiu, M., Ma, Q., et al. (2017). Hierarchical Specification of Pruriceptors by Runt-Domain Transcription Factor Runx1. J. Neurosci. *37*, 5549–5561.

Rattner, A., Smallwood, P.M., Williams, J., Cooke, C., Savchenko, A., Lyubarsky, A., Pugh, E.N., and Nathans, J. (2001). A photoreceptor-specific cadherin is essential for the structural integrity of the outer segment and for photoreceptor survival. Neuron *32*, 775–786.

Ren, A.J., Wang, K., Zhang, H., Liu, A., Ma, X., Liang, Q., Cao, D., Wood, J.N., He, D.Z., Ding, Y.Q., et al. (2014). ZBTB20 regulates nociception and pain sensation by modulating TRP channel expression in nociceptive sensory neurons. Nat. Commun. *5*, 4984.

Ross, S.E., McCord, A.E., Jung, C., Atan, D., Mok, S.I., Hemberg, M., Kim, T.K., Salogiannis, J., Hu, L., Cohen, S., et al. (2012). Bhlhb5 and Prdm8 form a repressor complex involved in neuronal circuit assembly. Neuron *73*, 292–303.

Saka, Y., Hagemann, A.I., Piepenburg, O., and Smith, J.C. (2007). Nuclear accumulation of Smad complexes occurs only after the midblastula transition in *Xenopus*. Development *134*, 4209–4218.

Shannon, P., Markiel, A., Ozier, O., Baliga, N.S., Wang, J.T., Ramage, D., Amin, N., Schwikowski, B., and Ideker, T. (2003). Cytoscape: a software environment for integrated models of biomolecular interaction networks. Genome Res. *13*, 2498–2504.

Shibata, S., Yasuda, A., Renault-Mihara, F., Suyama, S., Katoh, H., Inoue, T., Inoue, Y.U., Nagoshi, N., Sato, M., Nakamura, M., et al. (2010). Sox10-Venus mice: a new tool for real-time labeling of neural crest lineage cells and oligodendrocytes. Mol. Brain *3*, 31.

Sive, H.L., Grainger, R.M., and Harland, R.M. (2000). Early Development of *Xenopus laevis*. A Laboratory Manual (Cold Spring Harbor Laboratory Press).

Skarnes, W.C., Rosen, B., West, A.P., Koutsourakis, M., Bushell, W., Iyer, V., Mujica, A.O., Thomas, M., Harrow, J., Cox, T., et al. (2011). A conditional knockout resource for the genome-wide study of mouse gene function. Nature *474*, 337–342.

Sun, Y., Dykes, I.M., Liang, X., Eng, S.R., Evans, S.M., and Turner, E.E. (2008). A central role for Islet1 in sensory neuron development linking sensory and spinal gene regulatory programs. Nat. Neurosci. *11*, 1283–1293.

Thélie, A., Desiderio, S., Hanotel, J., Quigley, I., Van Driessche, B., Rodari, A., Borromeo, M.D., Kricha, S., Lahaye, F., Croce, J., et al. (2015). Prdm12 specifies V1 interneurons through cross-repressive interactions with Dbx1 and Nkx6 genes in *Xenopus*. Development *142*, 3416–3428.

Topilko, P., Schneider-Maunoury, S., Levi, G., Baron-Van Evercooren, A., Chennoufi, A.B.Y., Seitanidou, T., Babinet, C., and Charnay, P. (1994). Krox-20 controls myelination in the peripheral nervous system. Nature *371*, 796–799.

Usoskin, D., Furlan, A., Islam, S., Abdo, H., Lönnerberg, P., Lou, D., Hjerling-Leffler, J., Haeggström, J., Kharchenko, O., Kharchenko, P.V., et al. (2015). Unbiased classification of sensory neuron types by large-scale single-cell RNA sequencing. Nat. Neurosci. *18*, 145–153.

Xiang, M., Gan, L., Zhou, L., Klein, W.H., and Nathans, J. (1996). Targeted deletion of the mouse POU domain gene Brn-3a causes selective loss of neurons in the brainstem and trigeminal ganglion, uncoordinated limb movement, and impaired suckling. Proc. Natl. Acad. Sci. USA *93*, 11950–11955.

Yang, C.-M., and Shinkai, Y. (2013). Prdm12 is induced by retinoic acid and exhibits anti-proliferative properties through the cell cycle modulation of P19 embryonic carcinoma cells. Cell Struct. Funct. *38*, 197–206.

Young, G.T., Gutteridge, A., Fox, H., Wilbrey, A.L., Cao, L., Cho, L.T., Brown, A.R., Benn, C.L., Kammonen, L.R., Friedman, J.H., et al. (2014). Characterizing human stem cell-derived sensory neurons at the single-cell level reveals their ion channel expression and utility in pain research. Mol. Ther. *22*, 1530–1543.

Zhou, X., Wang, L., Hasegawa, H., Amin, P., Han, B.-X., Kaneko, S., He, Y., and Wang, F. (2010). Deletion of PIK3C3/Vps34 in sensory neurons causes rapid neurodegeneration by disrupting the endosomal but not the autophagic pathway. Proc. Natl. Acad. Sci. USA *107*, 9424–9429.

Zirlinger, M., Lo, L., McMahon, J., McMahon, A.P., and Anderson, D.J. (2002). Transient expression of the bHLH factor neurogenin-2 marks a subpopulation of neural crest cells biased for a sensory but not a neuronal fate. Proc. Natl. Acad. Sci. USA *99*, 8084–8089.

Zou, M., Li, S., Klein, W.H., and Xiang, M. (2012). Brn3a/Pou4f1 regulates dorsal root ganglion sensory neuron specification and axonal projection into the spinal cord. Dev. Biol. *364*, 114–127.

Zurborg, S., Piszczek, A., Martínez, C., Hublitz, P., Al Banchaabouchi, M., Moreira, P., Perlas, E., and Heppenstall, P.A. (2011). Generation and characterization of an Advillin-Cre driver mouse line. Mol. Pain *7*, 66.

STAR★METHODS

KEY RESOURCES TABLE

REAGENT or RESOURCE	SOURCE	IDENTIFIER
Antibodies		
Rabbit polyclonal anti-PRDM12	This paper	N/A
Guinea pig polyclonal anti-PRDM12	This paper	N/A
Rabbit polyclonal anti-PRDM12	Atlas Antibodies	Cat# HPA043143; RRID:AB_10806379
Guinea pig polyclonal anti-Runx1	Gift from Thomas Jessell	N/A
Mouse monoclonal anti-Runx3	Abcam	Cat# ab135248
Mouse monoclonal anti-Islet1	DSHB	Cat# 39.4D5; RRID:AB_2314683
Rabbit polyclonal anti-cleaved caspase 3	Cell Signaling	Cat# 9661; RRID:AB_2341188
Rabbit polyclonal anti-TrkA	Millipore	Cat# 06-574; RRID:AB_310180
Goat polyclonal anti-TrkA	R and D Systems	Cat# AF175; RRID:AB_354970
Goat polyclonal anti-TrkB	R and D Systems	Cat# AF1494; RRID:AB_2155264
Goat polyclonal anti-TrkC	R and D Systems	Cat# AF1404; RRID:AB_2155412
Rabbit polyclonal anti-DsRed	Clontech Laboratories	Cat# 632496; RRID:AB_10013483
Rabbit polyclonal anti-Nav1.8	Abcam	Cat# ab63331; RRID:AB_1142749
Rabbit polyclonal anti-Peripherin	Millipore	Cat# AB1530; RRID: AB_90725
Rabbit polyclonal anti-Histone H3	Millipore	Cat# 07-690; RRID: AB_417398
Mouse monoclonal anti-Pax3	DSHB	Cat# PAX3; RRID:AB_528426
Mouse monoclonal anti-Lhx3	DSHB	Cat# 67.4E12; RRID:AB_2135805
Rabbit polyclonal anti-GFP	Molecular Probes	Cat# A-6455; RRID:AB_221570
Goat anti-rabbit IgG, Alexa Fluor 488 conjugated	Molecular Probes	Cat# A-11008; RRID:AB_143165
Goat anti-rabbit IgG, Alexa Fluor 594 conjugated	Molecular Probes	Cat# A-11012; RRID:AB_141359
Donkey anti-goat IgG, Alexa Fluor 594 conjugated	Molecular Probes	Cat# A-11058; RRID:AB_142540
Goat anti-guinea pig IgG, Alexa 488 conjugated	Molecular Probes	Cat# A-11073; RRID:AB_142018
Goat anti-mouse IgG, Alexa 488 conjugated	Molecular Probes	Cat# A-11029; RRID:AB_138404
Goat anti-mouse IgG, Alexa 594 conjugated	Molecular Probes	Cat# A-11005; RRID:AB_141372
Biological Samples		
CS12 human embryonic sections	Joint MRC/Wellcome Trust (MR/R006237/1) Human Developmental Biology Resource	HDBR; http://www.hdbr.org
Chemicals, Peptides, and Recombinant Proteins		
Citral	Merck	Cat# C83007
Dexamethasone	Merck	Cat# D4902
Doxycycline hyclate	Merck	Cat# D9891
Critical Commercial Assays		
TruSeq RNA Sample Prep Kit v2	Illumina	Cat# RS-122-2001; RS-122-2002
Deposited Data		
RNA-seq data	This paper	GEO: GSE118187
Experimental Models: Cell Lines		
Cellectis-MCL	Ordovás et al., 2015	N/A
PRDM12-RMCE	This paper	N/A

(*Continued on next page*)

Continued		
REAGENT or RESOURCE	SOURCE	IDENTIFIER
Experimental Models: Organisms/Strains		
Prdm12$^{LacZ/+}$ mice	This paper; Genoway, project ID 84789	N/A
Prdm12$^{flox/flox}$ mice	This paper; Genoway, project ID 84789	N/A
Sox10-Venus mice	Shibata et al., 2010	N/A
Ngn1$^{GFP/+}$:Neurog1^{tm1And}/Neurog1^{tm1And} mice	Ma et al., 1998	RRID:MGI:3527491
Advillin-Cre: B6.129P2-Avil$^{tm2(cre)Fawa}$/J mice	Zhou et al., 2010	Cat# JAX:032536; RRID: IMSR_JAX:032536
Xenopus laevis	CRB (Centre de Ressources Biologiques Xénopes), Rennes University (France)	https://xenopus.univ-rennes1.fr/le-crb-xenopes
Oligonucleotides		
Primers for RT-qPCR experiments, Table S2	This paper	N/A
Software and Algorithms		
Cytoscape 3.4.0	Shannon et al., 2003	https://cytoscape.org
ClueGo 2.3.2		http://apps.cytoscape.org/apps/cluego
GraphPad Prism 6	GraphPad	SCR_002798
Star Alignment software 2.3.0e	Dobin et al., 2013	https://bioweb.pasteur.fr/packages/pack@STAR@2.3.0e
SAMtools 0.0.18	Li et al., 2009	http://samtools.sourceforge.net/
R/Bioconductor	Bioconductor	https://bioconductor.org/
DEseq2 1.8.2	Anders and Huber, 2010	http://bioconductor.org/

CONTACT FOR REAGENT AND RESOURCE SHARING

Further information and request for resources and reagents should be directed to and will be fulfilled by the Lead Contact, Eric Bellefroid (ebellefr@ulb.ac.be).

EXPERIMENTAL MODEL AND SUBJECT DETAILS

Mice

All mice were maintained on a C57BL/6J background and mice of either sex were used. Mice were provided *ad libitum* with standard mouse lab pellet food and water and housed at room temperature with a 12h light/dark cycle. The experimental protocols were approved by the CEBEA (Comité d'éthique et du bien être animal) of the IBMM-ULB and conformed to the European guidelines on the ethical care and use of animals.

For the generation of *Prdm12*$^{LacZ/+}$ mice, the European Mouse Mutant Cell Repository (EUCOMM) construct HTGR03016_Z_6_A08 was used. One of the homology arm was slightly shortened to favor the screening of ES cells after electroporation and five ES clones were obtained that underwent the expected recombination as determined by Southern blot analysis. One of these clone was used and injected into blastocysts (Genoway, project ID 84789). Chimeric mice were crossed with C57BL/6J individuals to generate the heterozygous *Prdm12*$^{LacZ/+}$ mice. *Prdm12* cKO mice were generated by first crossing our *Prdm12*$^{LacZ/+}$ mice with ROSA26-Flp mice in order to excise the *LacZ* cassette framed by *Frt* sites and obtain an allele with floxed exon 2. After further breeding to isolate the *Prdm12* floxed allele from the ROSA26-Flp allele, female *Prdm12*$^{flox/flox}$ mice were mated with *Advillin*-Cre males to generate cKO *Prdm12*$^{\Delta 2/\Delta 2}$ individuals (Zhou et al., 2010). *Sox10*-Venus mice were a gift from S. Shibata (Keio University, Japan) and were described elsewhere (Shibata et al., 2010). *Ngn1* knock-in GFP mice were a gift from François Guillemot and were described elsewhere (Ma et al., 1998).

PCR genotyping was used to detect the transgenic alleles. *LacZ* allele was detected using the primers Forward 5′-AGTTTGTA CATTCCCTGGGAGTAAGACTCC-3′ and Reverse 5′-AGCCAGGGGAAGAATGTGAGTTGC −3′. *Flp* allele was detected using the primers Forward 5′- CACTGATATTGTAAGTAGTTTGC-3′ and Reverse 5′- CTAGTGCGAAGTAGTGATCAGG-3′. *Prdm12* floxed allele was detected using primers Forward 5′- GCTGATCGAGTCCAGGAGAC-3′ and Reverse 5′- CCAAACATCCACAACCTTCA-3′. *Advillin-cre* allele was detected using the primers Forward 5′-GCTCGACCAGTTTAGTTACCC-3′ and Reverse 5′-TCGCGATT ATCTTCTATATCTTCAG-3′. *Sox10-Venus* transgene was detected using the primers Forward 5′- AAGACGTGGAGGCGGG ACGC-3′ and Reverse 5′- CACCACCCCGGTGAACAGCTCC −3′. For *Ngn1* knock-in GFP mice a common Reverse 5′- CCTGTACAT AACCTTCGGGC −3′ primer was used to detect WT and GFP allele with a WT Forward 5′- TGGTGTCGTCGGGGAACGAG −3′ primer or a GFP Forward 5′- AAGGCCGACCTCCAAACCTC −3′ primer.

Frogs

Xenopus laevis embryos were obtained from adult female frogs by induced hormone egg-laying and *in vitro* fertilization with crushed testicles collected from previously decapitated male individuals, using standard methods (Sive et al., 2000). The experimental protocols were approved by the CEBEA (Comité d'éthique et du bien-être animal) of the IBMM-ULB and conformed to the European guidelines on the ethical care and use of animals.

PRDM12-RMCE cell line

The ChiPSC6b iPSC line was purchased from Cellartis-Takara (Y11032 DEF-hiPSC ChiPSC6B), and maintained using E8 Flex (Life Technologies, A2858501) on Matrigel (Corning® Matrigel® Basement Membrane Matrix, growth factor reduced (GFR), VWR 734-0269). The Cellectis-Master Cell Line (Cellectis-MCL) containing heterotypic Flippase recognition target sequences integrated at its AAVS1 locus was generated as previously described (Ordovás et al., 2015).

The gBlock encoding human *PRDM12* cDNA was ordered from IDT, and inserted into the pZ:F3-P TetOn 3f-tdT-F recombinase-mediated cassette exchange (RMCE) donor vector for inducible expression (Ordovás et al., 2015), linearized with AflII and MluI using isothermal assembly (NEBuilder® HiFi DNA Assembly Master Mix, NEB E2621). The resulting pZ M2rtTA_CAGG TetON-*PRDM12* RMCE vector was co-nucleofected with a Flippase expression vector into the Cellectis-MCL to generate the *PRDM12*-RMCE line, as previously described (Ordovás et al., 2015).

SNP profiling of the original ChiPSC6b iPSC line was done in our lab, the established profile was later used to verify the identity of the gene engineered modified lines generated from the original cell line.

Cells were cultured and maintained at 37°C with 5% CO_2 and were of male gender.

Human embryonic samples

The CS12 human embryonic and fetal material was provided by the Joint MRC/Wellcome Trust (MR/R006237/1) Human Developmental Biology Resource (Gerrelli et al., 2015) (HDBR; http://www.hdbr.org). HDBR is regulated by the Human Tissue Authority and operates in accordance with the relevant codes of practice. Embryos were collected from women undergoing social termination of pregnancy with appropriate maternal written consent and approval from the Newcastle and North Tyneside NHS Health Authority Joint Ethics Committee. The samples were staged using the guidelines of Bullen and Wilson (1997), fixed in methacarn (60% absolute methanol, 30% chloroform, 10% glacial acetic acid) and processed through to paraffin wax (fibrowax, VWR). Sections were taken on a microtome at 7 μm thickness and mounted on Superfrost Plus microscope slides (Thermo Scientific). The karyotype of the embryo included in this study indicated that it was a male.

METHOD DETAILS

ISHs and immunostainings

Tissue dissection and preparation for ISH and immunostaining was performed as previously described (Thélie et al., 2015). *Prdm12 exon 2, Mpz, Vsx2, Evx1* and *Evx2* templates were PCR generated and primers for synthesis of *T7* containing templates can be communicated on request. Plasmids containing probe for mouse *Prdm12* (Kinameri et al., 2008), *Engrailed-1* (Joyner and Martin, 1987), *Neurogenin-1, Ntrk1, Ntrk2, Ntrk3* (Ma et al., 1999), *Ret* (Chen et al., 2006), *Scn10a, TrpM8, Zbtb20* (Ren et al., 2014), *Cdhr1* (Rattner et al., 2001), *Rgs4* (Hoekstra et al., 2013), *Neurod1* (Cau et al., 1997), *Tlx2* (Hatano et al., 1997), *Nhlh1* (Mattar et al., 2008), *Brn3a* (Sun et al., 2008) and *Krox20* (Ohayon et al., 2015) were described elsewhere. The *Xenopus laevis Ntrk1*, *Ntrk2* and *Ntrk3* probes were cloned by PCR from tailbud stage cDNA using the following primers: *Ntrk1* forward 5′-CTGGTTTGGAA CATGCTGGGC-3′ and *Ntrk1* reverse 5′-TTACTCCAAGATGTCTAAGTATACTGGTGG-3′; *Ntrk2* forward 5′- ATGCGCCTCTGGAAA GGTTC −3′ and *Ntrk2* reverse 5′- TCTTGCTCCAAATGAAATCTGTCTCAC −3′; *Ntrk3* forward 5′- ATGGATGTGTGGCTTGTCC CT −3′ and *Ntrk3* reverse 5′- TTGGTGGAGGATTCCCAAGCA −3′. The PCR products were then cloned into the pGemT easy vector (Promega) and the riboprobe synthesized (SacII, SP6). *In situ* plasmids for *Xenopus Prdm12* (Thélie et al., 2015), *Tubb2b* (Oschwald et al., 1991), *Xhe* (Hong and Saint-Jeannet, 2007) and *Foxi1c* (Jaurena et al., 2015) were described elsewhere. ISH experiments were performed as previously described using antisense digoxigenin-labeled riboprobes (Thélie et al., 2015).

Primary antibodies used were: homemade rabbit and guinea pig anti-PRDM12 (respectively 1:5000 and 1:2000), rabbit anti-PRDM12 (1:100; Atlas Antibodies, HPA043143), guinea pig anti-Runx1 (1:8000; gift from Dr. Thomas Jessell), mouse anti-Islet-1 (1:200; DSHB, 39.4D5), rabbit anti-cleaved Caspase-3 (1:1000; Cell Signaling, #9661), rabbit anti-TrkA (1:500; Millipore, 06574), goat anti-TRKA (1:100; R&D Systems, AF175), goat anti-TrkB (1:500; R&D Systems, AF1494), goat anti-TrkC (1:500; R&D Systems, AF1404), rabbit anti-tdTomato (1:400; Clontech, #632496), rabbit anti-Nav1.8 (1:500; Abcam, ab63331) mouse anti-Pax3 (1:200; DSHB), mouse anti-Lhx3 (1:1000; DSHB), rabbit anti-GFP (1:1000; Invitrogen, A6455). Fluorescence acquisition of the Venus protein carried by *Sox10*-Venus embryos as presented in the data corresponded to endogenous fluorescence signal. Secondary antibodies used were: anti-rabbit Alexa488 (Invitrogen, A11008), anti-rabbit Alexa594 (Invitrogen, A11012), anti-goat Alexa594 (Invitrogen, A11058), anti-guinea pig Alexa 488 (Invitrogen, A11073), anti-guinea pig Alexa488 (Bio-connect), anti-mouse Alexa488 (Invitrogen, A11029), anti-mouse Alexa594 (Invitrogen, A11005). Immunostaining experiments were performed as previously described (Thélie et al., 2015). Images collection and analysis were performed using a wide-field fluorescence microscope

Zeiss Axio Observer Z1, a laser-scanning confocal microscope Zeiss LSM 710 using the Zeiss Zen microscopy software or a stereo microscope Olympus SZX16 and the softwares Cell^F or CellSens Entry V2.1.

Rabbit and guinea pig anti-PRDM12 antibodies

A truncated *Prdm12* coding sequence corresponding to amino acids 45 to 203 of the human PRDM12 protein was cloned into the pET15b vector following a N-terminal polyhistidine (6xHis) tag sequence. Generation and purification of the protein used for immunization was performed by immobilized metal affinity chromatography (IMAC), size exclusion and ion exchange chromatography at the VBCF Protein Technologies Facility (https://www.viennabiocenter.org/facilities/). Rabbit immunization and collection of sera was performed by Diagenode (https://www.diagenode.com/). Guinea pig immunization and collection of sera was performed by Eurogentec (https://secure.eurogentec.com/eu-home.html).

Whole-mount X-gal staining of embryos

Embryos were fixed in 4% PFA for one hour at room temperature and rinsed in detergent solution (2mM $MgCl_2$, 0.01% sodium deoxycholate, 0.02% NP-40 diluted in 0.1 M pH 7.3 phosphate buffer). Embryos were then incubated at 37°C in staining solution composed of detergent solution with 5mM $K_3Fe(CN)_6$, 5mM $K_4Fe(CN)_6$ and 1mg/ml of X-gal. Prior to clearing embryos were progressively dehydrated in increasing concentrations of methanol. After several washes in 100% methanol embryos were incubated in a solution of methanol:BABB (1:1) before being incubated and stored in 100% BABB. BABB is made of one part of benzyl alcohol for two parts of benzyl benzoate.

Xenopus embryo microinjections and AC assays

The *Xenopus Prdm12, Ngn1, Ngn2, Ngn2-GR*, *Pax3-GR* and *Zic1-GR* expression vectors and templates were described elsewhere (Hong and Saint-Jeannet, 2007; Nieber et al., 2009; Perron et al., 1999; Thélie et al., 2015). Synthetic mRNAs were made using Sp6 mMessage mMachine (Ambion). *Xenopus laevis* embryos were staged according to Faber and Nieuwkoop (1994). For ISH analyses, embryos were injected in one cell of two- to four-cell-stage embryos. In all experiments, embryos were co-injected with lacZ mRNA (50 pg/blastomere), and β-gal activity was revealed by X-gal staining (in light blue). For AC explant assays, synthesized mRNA was microinjected into the animal region of each blastomeres of four-cell stage embryos. ACs were dissected at blastula stage (St.9) and cultured in 1X Steinberg medium, 0.1% BSA until sibling embryos reach the appropriate stage. For experiments including GR fused constructs, dissected explants were directly harvested in culture medium containing 10 μM of dexamethasone. To determine the non-cell autonomous effect of Zic1 on *Prdm12* expression, 100 μM of citral (Sigma-Aldrich), an inhibitor of retinoic acid synthesis, was added to the culture medium of *Zic1-GR* mRNA injected AC explants together with dexamethasone.

Differentiation of human pluripotent stem cells to nociceptors

The optimized differentiation protocol for hPSCs toward nociceptors was adapted from previous studies (Chambers et al., 2012; Young et al., 2014), and consists of three stages: neural induction by dual SMAD inhibition using LDN193189 and SB-431542 to drive anterior neuroectoderm specification from Day 1 to 5, then sensory neuron specification using the GSK3 inhibitor CHIR99021, the gamma-secretase complex inhibitor DAPT, and the fibroblast growth factor receptor inhibitor SU5402 from Day 5 to 10, followed by sensory neuron maturation with BDNF, GDNF, NT3, Ascorbic Acid, and NGF from Day 10 to 25.

The nociceptor phenotype of the resulting cells was verified following by RT-qPCR the expression of *B3TUBB*, *BRN3A*, *GAPDH*, *ISL1*, *KLF7*, *NTRK1*, *NTRK2*, *NTRK3*, *PRDM12*, *RUNX1*, *TAC1*, *TRPA1*, *TRPM3*, *TRPM8*, *TRPV1*, *TRPV4* was assessed by qPCR. The *PRDM12*-RMCE line was treated with 3 μg/ml doxycycline from Day 7 till Day 25 to induce expression of *PRDM12*.

Real-time RT-qPCR

Real-time RT-qPCR analysis were performed as reported (Hanotel et al., 2014). RT-qPCR data were collected using a StepOnePlus Real-Time PCR System machine and the related StepOne Software v2.3. Gene expression levels in *Xenopus* AC and human iPSC assays were normalized using the ΔΔCt method. Expression levels were first normalized with the level of *GAPDH* expression and then, for *Xenopus* assays with the level of target gene expression in naive uninjected caps (defined as 1) or, for human iPSCs, with the level of target gene expression in human iPSCs without overexpression of *PRDM12* at the corresponding day of differentiation (defined as 1). The expression level of *Prdm12 exon 1-5* in mouse embryos was normalized using the ΔCt method with the level of *GAPDH* expression as a reference. Gene expression levels reported for each biological replicate correspond to the mean value of at least a technical duplicate. The respective level of expression for each exon observed in wild-type individuals was defined as 100% of expression. Bar plots were generated using GraphPad Prism and represent the mean ± SEM of biological replicates. Primer pairs used to monitor gene expression are listed in Table S2.

Human embryo immunostainings

Sections were dewaxed with Histo-Clear (National Diagnostics), rehydrated in graded ethanol and rinsed in distilled water. Antigen retrieval was performed by heating the sections to 95°C in sodium citrate buffer pH 6 for 20 minutes. Cooled sections were rinsed in distilled water before two times five minute permeabilization washes in Tris-HCL 0.1% Triton buffer pH 10 (Tris-HCL-T buffer). To

prevent non-specific staining, sections were blocked in 10% donkey serum and 10% IHC blocking buffer (Sigma) diluted in Tris-HCL-T buffer for 90 mins. Sections were incubated overnight at 4°C in a humidified chamber with goat polyclonal anti-TRKA antibody (above) and rabbit polyclonal anti-PRDM12 (above), diluted in Tris-HCL-T buffer containing 10% donkey serum. After washing with Tris-HCL-T buffer, sections were labeled for 2 hours at room temperature with anti-goat IgG-488 (Invitrogen) and anti-rabbit IgG-546 (Invitrogen). Slides were washed with Tris-HCL buffer and mounted using Fluromount-G DAPI (Invitrogen). Specimens were visualized using the Zeiss LSM780, confocal microscope system.

RNA sequencing and data processing

For sequencing, the RNA-samples were prepared with the "TruSeq RNA Sample Prep Kit v2" according to the manufacturer's protocol (Illumina). Single read (50 bp) sequencing was conducted using a HiSeq 2000 (Illumina). Four independent biological replicates were analyzed for the E11.5 KO and WT conditions. One of the four KO samples was later excluded from the analysis as it was defined as an outlier based on clustering and PCA analysis. Sequence images were transformed to BCL files with the Illumina BaseCaller software and samples were demultiplexed to FASTQ files with CASAVA (version 1.8.2). Sequencing quality was checked and approved using the FastQC software (http://www.bioinformatics.babraham.ac.uk/projects/fastqc/). Sequences were aligned to the genome reference sequence of *Mus musculus.* Alignment was performed using the STAR alignment software (Dobin et al., 2013) (version 2.3.0e) allowing for 5 mismatches within 50 bases. Subsequently, conversion of resulting SAM files to sorted BAM files, filtering of unique hits and counting was conducted with SAMtools (Li et al., 2009) (version 0.1.18) and featureCounts (version 1.4.6-p1). Data was preprocessed and analyzed in the R/Bioconductor environment (http://www.bioconductor.org/) using the DEseq2 package (Anders and Huber, 2010) (version 1.8.2). Specifically, the data were normalized and tested for differentially expressed genes based on a generalized linear model likelihood ratio test assuming negative binomial data distribution. Candidate genes were filtered based on a FDR-corrected p value < 0.05.

Gene ontology analysis was performed using Cytoscape 3.4.0 (Shannon et al., 2003) with the plug-in ClueGo 2.3.2 (Bindea et al., 2009). Genes for the analysis were sorted based on a FDR-corrected p value < 0.05 and a $\log_2|0.25|$ of fold change. The murine GO Biological Process (version from 23 February 2017) was used with the following settings: Evidence code, All; GO Term fusion; GO Tree Interval, 6 to 13; Pathways with p value ≤ 0.05; GO Term Selection, 2 and 5%.

QUANTIFICATION AND STATISTICAL ANALYSIS

Statistical analysis

GraphPad Prism version 6 was used for statistical analyzes included in the main and supplementary figures of the study. Statistical tests used are specified in the figure legends wherever appropriate. No statistical methods were used to predetermine sample sizes, but our sample sizes are similar to those from the field.

Replications

All experiments were replicated a number of times depending of the experiment performed. For qualitative data such as those obtained from ISH and immunohistochemistry, pictures are representative of what was observed in at least three independent samples. Graphical quantifications derived from qualitative data indicate the number (n) of embryos included in the analysis (which are plotted as individual values whenever possible); mean ± SD is also reported. RT-qPCR data are presented as the mean ± SEM of at least two independent experiments (which are plotted as individual values whenever possible). *Xenopus laevis* RT-qPCR experiments were performed on pools of 30-50 AC explants per condition.

Randomization

No randomization was performed in this study.

Mouse samples were allocated to experiments depending on their genotype that resulted in the comparison of samples from genetically modified mouse lines with homozygous genetic deletion to control or WT littermates.

For experiments performed on *Xenopus laevis* embryonic samples, the different groups are clearly defined in the study and consist in embryos/AC explants injected with a defined combination of mRNA and control samples that were not injected.

For induced pluripotent stem cells, the different groups were defined based on the time of differentiation and the addition or not of doxycyline to the culture medium.

DATA AND SOFTWARE AVAILABILITY

RNA-seq data have been deposited at GEO under accession GSE118187.